Development of Microfabrication Technologies on Oil-based Sealing Devices for Single Cell Metabolic Analysis

by

Ganquan Song

A Dissertation Presented in Partial Fulfillment
of the Requirements for the Degree
Doctor of Philosophy

Approved April 2017 by the
Graduate Supervisory Committee:

Deirdre R. Meldrum, Chair
Michael Goryll
Laimonas Kelbauskas
Hong Wang

ARIZONA STATE UNIVERSITY

May 2017

ABSTRACT

In the past decades, single-cell metabolic analysis has been playing a key role in understanding cellular heterogeneity, disease initiation, progression, and drug resistance. Therefore, it is critical to develop technologies for individual cellular metabolic analysis using various configurations of microfluidic devices. Compared to bulk-cell analysis which is widely used by reporting an averaged measurement, single-cell analysis is able to present the individual cellular responses to the external stimuli. Particularly, oxygen consumption rate (OCR) and extracellular acidification rate (ECAR) are two key parameters to monitor heterogeneous metabolic profiles of cancer cells. To achieve multi-parameter metabolic measurements on single cells, several technical challenges need to be overcome: (1) low adhesion of soft materials micro-fabricated on glass surface for multiple-sensor deposition and single-cell immobilization, e.g. SU-8, KMPR, etc.; (2) high risk of using external mechanical forces to create hermetic seals between two rigid fused silica parts, even with compliance layers; (3) how to accomplish high-throughput for single-cell trapping, metabolic profiling and drug screening; (4) high process cost of micromachining on glass substrate and incapability of mass production.

In this dissertation, the development of microfabrication technologies is demonstrated to design reliable configurations for analyzing multiple metabolic parameters from single cells, including (1) improved KMPR/SU-8 microfabrication protocols for fabricating microwell arrays that can be integrated and sealed to 3 × 3 tri-color sensor arrays for OCR and ECAR measurements; (2) design and characterization of a microfluidic device enabling rapid single-cell trapping and hermetic sealing single cells and tri-color sensors

within 10 × 10 hermetically sealed microchamber arrays; (3) exhibition of a low-cost microfluidic device based on plastics for single-cell metabolic multi-parameter profiling. Implementation of these improved microfabrication methods should address the aforementioned challenges and provide a high throughput and multi-parameter single cell metabolic analysis platform.

ACKNOWLEDGMENTS

I would like to express my sincere gratitude to Arizona State University for letting me fulfill my dream of being a graduate student here. I would also like to thank the Center for Biosignatures Discovery Automation for providing me the opportunity to work on very interesting and novel projects. To my committee, Dr. Deirdre Meldrum, Dr. Michael Goryll, Dr. Hong Wang, and Dr. Laimonas Kelbauskas, I am extremely grateful for your patient guidance and inspiring suggestions throughout my research. To Dr. Yanqing Tian and Dr. Fengyu Su, thank you for always supplying me brilliant sensor solutions to deposit sensor arrays and answering my endless questions. To Dr. Liqiang Zhang and Sandhya Gangaraju, thank you for culturing various types of cells for me every day. To Dr. Xiangxing Kong and Dr. Bin Cao, thank you for introducing me to the basic concepts of chemistry and optics. To Dr. Honor Glenn, thank you for helping me to use all the fluorescent microscopes for cell imaging. To Dean Smith, thank you for writing so many beautiful software for analyzing images. To Wacey Teller, thank you for drawing plenty of 3D images. To my colleagues, especially Rishabh Shetty, Meryl Rodrigues, Shufang Ci and Arthur Wang, thank you for giving me words of encouragement all the time to complete my projects. I would like to thank my parents, who brought me to the world and always tell me how to be a humble and dynamic person. Most of all, I am fully indebted to Dr. Deirdre Meldrum, my advisor and director, for your understanding, patience, enthusiasm, wisdom, and encouragement and for pushing me farther than I thought I could go.

TABLE OF CONTENTS

Page

CHAPTER Page

CHAPTER Page

CHAPTER Page

LIST OF TABLES

Table Page

LIST OF FIGURES

Figure Page

Figure Page

Figure Page

Figure Page

Figure Page

1. INTRODUCTION

Cellular heterogeneity is considered as a critical principle of cell biology in understanding many biological processes, such as carcinogenesis, proliferation and drug resistance (Lidstrom and Meldrum 2003, Cai, Friedman et al. 2006, Losick and Desplan 2008). Studies of cellular metabolic analysis have been developed progressively in recent years (Smallwood, Lee et al. 2014, Hyun, McElwee et al. 2015). Cellular function is correlated with stochastic expression of genes, proteins and metabolites, which have important consequences for cell-to-cell variability (Raj and van Oudenaarden 2008). Hence, studies of genetic and epigenetic variations among cell populations can cause differential cellular phenotypes (Irish, Kotecha et al. 2006). But there are a lot of barriers for further research on cellular analysis (Zhang, Cui et al. 1992). One of the most critical influences is the cellular microenvironment consisting of a complex dynamic system with numerous stochastic expression of genes (Losick and Desplan 2008), caused by the genetic and/or non-genetic heterogeneity in the cell (Kelbauskas, Ashili et al. 2012). To characterize cellular phenotypes, bulk cell measurements based on ensemble-averaged data are widely selected because they are simple and well-developed techniques for addressing intracellular molecules (Wheeler, Throndset et al. 2003). Although bulk cell measurements based on ensemble-averaged data are widely selected and well-developed to elucidate how cells respond to extracellular perturbations (Lidstrom and Konopka 2010), this analysis method can result in a misleading interpretation since the detection of some vital individual cellular processes is lost in the bulk average (Anselmetti 2009). For instance, it is impossible to characterize cellular parameters at an intermediate state since cells reacting

to the stimuli from distinct subpopulations are not a normal distribution (Krylov and Dovichi 2000). The more accurate representation to address intrinsic intercellular heterogeneity is to analyze the content of single cells with high spatiotemporal resolution, as the detailed information is crucial to explain the precise role of individual cells in complex multicellular organisms, study how they interact with their local microenvironments, and develop effective prescription for the diseases (Rosenfeld, Young et al. 2005, Wu, Neilson et al. 2007, Cairns, Harris et al. 2011).

Single-cell analysis (SCA) is a key factor to understanding cellular heterogeneity, carcinogenesis, proliferation, and drug resistance (Meldrum and Holl 2002, Lidstrom and Meldrum 2003). Individual cells have discrete molecular, metabolic, phenotypic and genetic identities, so they play distinctive roles in an organism because of cell-to-cell heterogeneity (Cornelison and Wold 1997). However, with this uncertain heterogeneity, it brings difficulties in studying the precise etiology and developing effective prescription for the disease, so methods of analyzing single cells help to understand how they interact with their local microenvironments for cellular diversity and heterogeneity (Irish, Kotecha et al. 2006). One important application of SCA is investigating cancer cells since cancer tumors consist of a group of different cells characterizing different properties (Cairns, Harris et al. 2011). The metabolism of most cancer cells is significantly different from that of normal cells, as cancer cells consume a small amount of oxygen and produce more hydrogen ions during respiration (Hsu and Sabatini 2008), since glycolysis and oxidative phosphorylation providing energy to cellular processes play an important role in sensitively reflecting alterations in physiologic state of cells and helping to detect disease status at single-cell level (Beckman, Schemmann et al. 2012). Particularly, single-cell analysis provides a new

and promising pathway to acquire a more in-depth knowledge on prevention and treatment of cancer (Mannello, Ligi et al. 2012). Experimental studies at the single-cell level including genomics, proteomics and metabolomics benefit to define the cell-to-cell heterogeneity, to characterize rare cells (e.g. cancer stem cells, and tumor initiating cells) and reveal their intra- and extra-cellular response to microenvironmental stimuli, and finally to identify personalized therapeutic strategies (Beckman, Schemmann et al. 2012). The known Warburg effect caused by oncogenic alterations is the underlying mechanism to understand malignant transformation in tumor cells, and it is sensitively reflected by changes in cellular metabolism and cellular microenvironment such as oxygen deficiency or production of lactate and other acids (Warburg, Wind et al. 1927, Dang and Semenza 1999). Therefore, the essential pathway to monitor the physiological state of living tumor cells and the effects of environmental perturbations on cell function is simultaneously measuring the rate of oxygen consumption and rate of extracellular acidification (Owicki and Parce 1992). Therefore, the two critical cellular parameters after glycolysis and oxidative phosphorylation, oxygen consumption rate (OCR) and extracellular acidification rate (ECAR) of single cells, indicate a pivotal approach to tell the difference between cancer cells and normal cells.

One commercial product to measure OCR and ECAR is the Oxygraph Plus System from Hansatech Instruments Ltd (Norfolk, UK), which can sensitively measure dissolved oxygen and pH in liquid-phase samples (bulk cells) in an electrode chamber. Another product, Seahorse XFp Analyzer, which is developed by Agilent Technologies Inc (Santa Clara, CA), is capable of measuring real-time OCR and ECAR of live cells in a microwell plate (as few as 5,000 cells per well) with high sensitivity. Although the two systems could

accurately and/or rapidly generate cellular metabolic phenotype for a large population of cells, the limitation of these methods is that the final analysis is based on the averaged measurements of bulk cells and some important and crucial individual cellular responses to the local environment is most likely lost in the averaging effects. To quantify the phenotypes including OCR and ECAR at the single cell level, it is of paramount importance to obtain dynamic monitoring of multiple individual cells and achieve high throughput analysis. Manipulation of microfluidics has emerged as a powerful and encouraging technology for exploring the inherent features of cellular systems, where typical microfluidic channels (10-100 μm) are comparable to the dimension of single cells (Whitesides 2006). To attain adequate response when very small target amounts are detected in a microsystem with extremely complicated components, microfluidics or "lab-on-a-chip" technology has been developed to perform high throughput analysis of single cells with minimal reagent consumption (Wheeler, Throndset et al. 2003), because they could integrate the basic and inevitable cellular processes (such as positioning, trapping or detection of target cells) on the micrometer scale. In addition, such lab-on-a-chip devices provide the capability to isolate individual cells or other analytes in hermetic microchambers (Chao and Ros 2008). The hermetic sealed structures allow and manipulate high throughput screening to obtain accurate detections on the independent individual cells which are not influenced by their neighbors. In the Center for Biosignatures Discovery Automation (CBDA), we developed several configurations based on "lid-on-top" structures (Kelbauskas, Ashili et al. 2012, Kelbauskas, Ashili et al. 2017, Kelbauskas, Glenn et al. 2017), which basically consisted of bottom microwells and top lids, sealed by mechanical force applied on the top of the configurations.

One important nontrivial aspect to develop single-cell metabolic analysis platform is to form reliable hermetically sealed microchambers of picoliter volumes that contain single cells and extracellular fluorescence sensors to sensitively measure real-time metabolic parameters of interest. Enclosing single cells in sealed microchambers offers a more unique, accurate and reliable measurement of oxygen consumption and pH change compared to using microprobe-based measurements (Bavli, Prill et al. 2016). Most of the published technical approaches are based on various lid-on-top configurations that form hermetically sealed microchambers by pressing a glass lid containing micropockets for optical sensor deposition to a bottom glass chip containing microwells for single-cell loading (Kelbauskas, Ashili et al. 2012, Song, Shetty et al. 2013). However, using glass as a substrate material could bring potential sealing problems to the structures, because they showed a relatively low tolerance to the appearance of unexpected particles between the two layers, even with a compliance layer of poly(dimethylsiloxane) (PDMS) or Parylene C (Rodrigo, Daria et al. 2004). In addition, it usually required a quite large (80 N) mechanical force applied to seal the top lid and bottom chip, which could generate severe cracks on both layers and lead to failure of hermetical sealing. To eliminate these potential leakage issues caused by particles and large mechanical force, soft materials are selected to be substrate materials instead of glass, such as PDMS and thick photoresists. Since PDMS layers are highly permeable to oxygen (Saito, Wu et al. 2006), negative photoresist materials (such as SU-8 and KMPR) with low oxygen permeability are more favorable to construct microfluidic channels and microwells in this lid-on-top configuration for cellular multi-parameter analysis. To avoid possible fractures on the top and bottom layers caused by mechanical forces, mineral oil having very low oxygen permeability can be used as a

sealing material (Zettlemoyer, Aronson et al. 1970) to isolate single cells from air and limit the diffusion into microchambers. A detailed design for single-cell metabolic profiling is demonstrated in Chapter 2.

In addition, the speed of cell loading by the home-built piezo-driven pico-pump was low as it took about 40 minutes to load 9 single cells. The pico-pump was developed in CBDA and could select and transfer individual cells to analysis locations by generating fluid pressure. To achieve 10 × 10 or larger matrix, microfluidic channels were designed to implement rapid cell loading. Mineral oil could be used as the sealing material in the channels since gas diffusion in mineral oil is two to three order lower than that in water (Rodrigues, 2014). The mechanism of the configuration was that the single cells in bulk solution flowing into the channels were immobilized by Pachinko-shaped traps, and assembled by a microwell array embedded with tri-color sensors. The formed micro-chambers were hermetically sealed by mineral oil and the sensor fluorescence intensities were collected on an inverted microscope. Most importantly, mineral oil could be dynamically displaced by cell culture media, where drug molecules mixed in the media could be introduced into the micro-chambers containing cells (Rodrigues, 2014). By analyzing the fluorescence intensities from tri-color sensors, the single cells' reactions to the drug were monitored in real-time, demonstrating the utility of the device for drug response screening on the same cells. The entire platform is described in Chapter 3.

The demonstrated techniques in Chapter 2 and 3 are based on glass materials for cell immobilization, which require large numbers of single-use chips especially for building cellular heterogeneity database. As process cost of fabricating glass chips in clean room is

considerable, plastics are selected as an alternative material to produce disposable chips for the single-cell metabolic profiling. When the micro-machined nickel mold was fabricated by deep silicon etch and electroplating, it was used for hot embossing for mass production. The plastic chips were used in the microfluidic device for single-cell metabolic analysis as described in Chapter 4.

Contributions of this PhD research:

1. Further developed and optimized an advanced microfluidic device to measure oxygen consumption and extracellular acidification at the single cell level in real time.

2. Optimized the use of mineral oil as a sealing material integrated into microfluidic devices.

3. Achieved a rapid way to load large numbers of live single cells.

4. Fabricated patterned chips using thermoplastic polymers with low processing time and cost.

5. Applied plastic materials in the single cell metabolic analysis.

6. Monitored live single cells' reactions to drug molecules on the device.

2. KMPR APPLICATION ON PHOTO-PATTERNED, TRI-COLOR FLUORESCENCE SENSOR ARRAYS FOR SINGLE-CELL MULTI-PARAMETER METABOLIC PROFILING

To investigate whether KMPR/SU-8 (negative photoresist) can be used in microfluidic devices for single cell metabolic profiling analysis, a backside exposure process to fabricate KMPR microwell arrays on fused silica substrates was developed. The probe to detect the single cells' metabolic parameters is a photo-patterned and polymerized optical tricolor sensor including oxygen, pH and Rhodamine (reference) probes, which can reflect the variation of oxygen concentration and pH value in the immediate microenvironment of individual cells. Since KMPR is a soft negative photoresist, microwell arrays made of KMPR have higher tolerance interference from foreign particles than glass-based microwells. The developed microfabrication method can provide a platform for simultaneously analyzing live cell respiration and other metabolic parameters at the single-cell, multiple-cell, and tissue level.

2.1 Introduction

The traditional live cell metabolic measurements based on bulk cells analysis from the earlier studies represent only averaged cellular responses to extracellular stimuli, leading to erroneous understandings of cell-to-cell heterogeneity (Meldrum and Holl 2002). Over the last years metabolic analysis of single cells has been recognized as the key technology for accurately explaining disease initiation, progression, and drug resistance (Lidstrom and Meldrum 2003). Among many metabolic parameters, extracellular acidification rate

(ECAR) and oxygen consumption rate (OCR) are two critical indicators of monitoring cellular metabolism (Lidstrom and Konopka 2010). To detect ECAR and OCR at the single-cell level, real-time monitoring systems with fmol/min measurement resolution that analyze single-cell metabolic parameters are becoming increasingly popular in the past decade (Molter, Holl et al. 2008).

Recent studies have reported fused silica based microfluidic devices fabricated using standard photolithography process (Zhu, Holl et al. 2009). Fluorescent optical sensors for measuring extra-cellular oxygen concentration, pH and other metabolic parameters were deposited on planar or microwell lids then hermetically sealed with single cells loaded bottom microwells for single-cell metabolic analysis (Kelbauskas, Ashili et al. 2012, Kelbauskas, Ashili et al. 2017, Kelbauskas, Glenn et al. 2017). One of the significant advantages of this "lid-on-top" configuration (**Figure 1**) is that the highly transparent cell-trapping platform fabricated on glass substrate can provide low auto-fluorescence noise, high chemical stability, reliable compatibility with microelectromechanical systems (MEMS) and facilitation of integration with the sensors (Zhu, Tian et al. 2012). However, the technical challenge of the method introduced above in metabolic profiling using fused silica as a substrate material is the potential of sealing problems affected by foreign particles between two rigid fused silica parts, even with a compliance layer of PDMS or Parylene C (Rodrigo, Daria et al. 2004). As shown in **Figure 2**(a) and (b), any particles trapped in between two fused silica parts not only could produce leakage in one single microwell, but also lead to failure of hermetical sealing of the whole chip.

To eliminate the leakage issues caused by particles, microwells fabricated using soft materials such as thick negative photoresists can be an effective solution. The fabricated pattern near the unexpected particles is deformed while other patterns on the same substrate were not affected by the particle when mechanical force is applied on the top lid to the bottom microwells for hermetical sealing (**Figure 2c**). Among all types of negative tone photoresists, KMPR and SU-8 (Microchem Corp., USA) are two of the most commonly used and well-known materials for their high aspect ratio features in biological applications (Lee and Jiang 2008). Although SU-8 is widely applied in the integration over various labs-on-a-chips (Peng, Ling et al. 2006), fissuring can be easily generated by internal stress created during the fabrication process (Shaw, Nawrocki et al. 2003) causing problematic sealing of the "lid-on-top" configuration. Compared to SU-8, KMPR has a higher resistance to fissuring (Ou, Yan et al. 2008), and, more importantly, superior moisture resistance (Kim, Park et al. 2004) which plays significant role in biocompatible application of microfluidic devices for single-cell analysis.

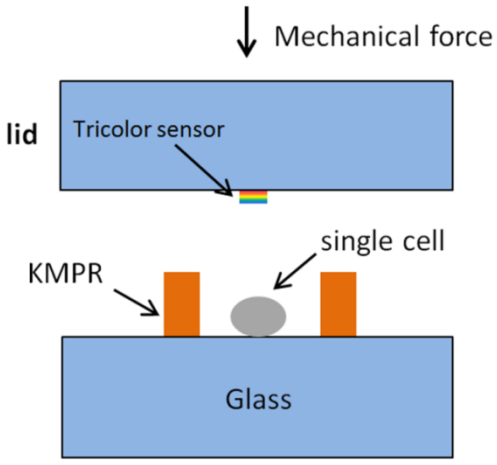

Figure 1. "Lid-on-top" Configuration.

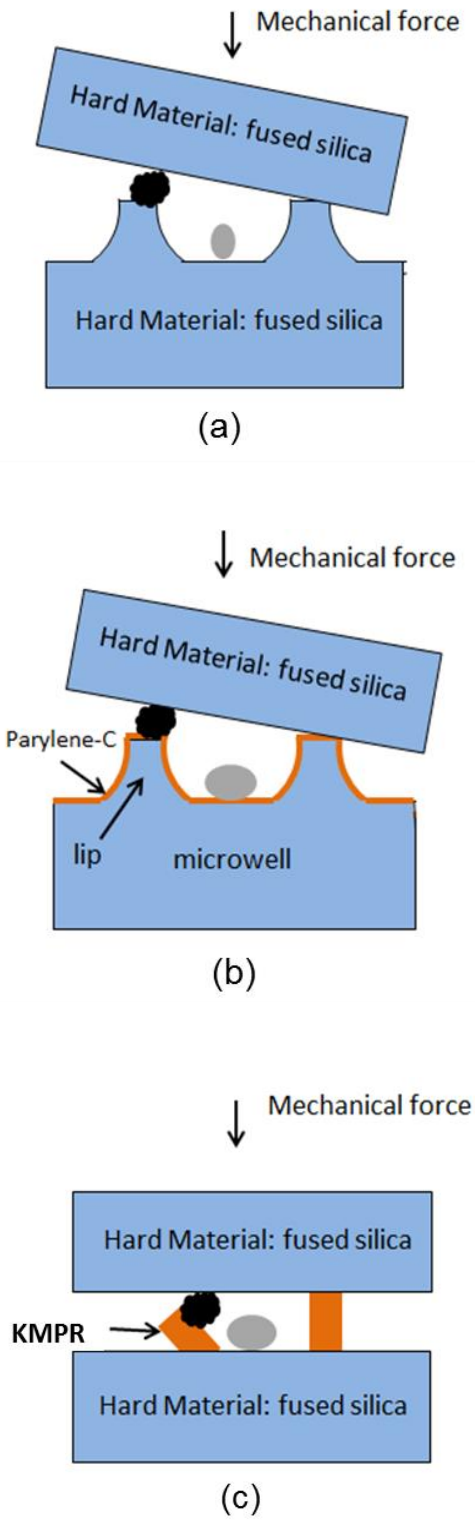

Figure 2. Particle Issue in Three Different Configuration Types: (a) Hard-Hard, (b) Hard-Compliance/Hard, and (c) Hard-Soft-Hard.

To successfully achieve ECAR and OCR measurements through mechanically sealing a fused silica lid and microwells with KMPR sidewalls containing single cells, the main challenge is the stability of the KMPR layer: moisture resistance to cell culture medium and physical resistance to the mechanical force applied during the process of sealing. Considering the thickness (~ 20 μm) of KMPR designed for the experiment, there is a difference between the UV exposure dose at the top of the resist and the bottom of the resist since KMPR absorbs energy from the UV light source (Blanco Carballo, Melai et al. 2008). The non-uniform UV exposure dose results in the fact that the top layer is overexposed and the bottom layer is relatively underexposed, and therefore the dimensions of the KMPR structures at the top and the bottom is not same after development: the top structure is generally wider than the structures at the bottom. It is a particularly serious concern when KMPR sidewalls are to withstand a large mechanical force, and even shear force is generated inadvertently (Ray, Zhu et al. 2010). A recent report introduced the backside exposure method of SU-8 to fabricate a reentrant structure (Peterman, Huie et al. 2003), which can be similarly applied in KMPR processing. As the backside exposure process enables the interface of KMPR layer and fused silica surface receiving the most energy to form truncated cone-shaped KMPR microwells, the method can micro-fabricate microwells with higher resistance to moisture and mechanical force which is necessary for single-cell metabolic analysis. On the fused silica lid, the photo-patterned tricolor sensor array consisting of an oxygen probe and a pH probe can be aligned and sealed with the KMPR microwells to measure the ECAR and OCR of the single cells.

In this chapter, metabolic profiling results of single cells hermetically sealed in KMPR microwells fabricated by using the backside exposure process are reported. The backside

exposure procedure is demonstrated to have better moisture resistance for single-cell analysis. The features of the fabricated KMPR microwells and photo-patterned tricolor sensors are characterized to understand the metabolic profiling results.

2.2 Experimental

2.2.1 Materials and Instrument

Four inch double side polished fused silica wafers (University Wafer, South Boston, MA) were selected as the substrate because of its optical transparency. A thin film layer of chrome was deposited onto the substrate as the hard masking material for backside exposure. Photoresist AZ3312 (Mays Chemicals, Indianapolis, IN) was used as masking layer for chrome etch by a commercially available chrome etchant. Photoresist KMPR® 1025 (Microchem Corp., Westborough, MA) was fabricated to arrays of microwells for photolithography. MF-26A developer (Microchem Corp., Westborough, MA) is used to develop KMPR® 1025 patterns on fused silica substrate. A polymerizable tricolor sensor (pH probe, oxygen-probe and reference-probe) was synthesized by the chemistry group led by Dr. Yanqing Tian in CBDA (Arizona State University, Biodesign Institute) and photo-patterned for the metabolic profiling. Trimethylsilylpropyl acrylate (TMSPA) is vapor deposited on a fused silica die for polymerization of tricolor sensors.

Edwards Auto 306 E-beam Evaporator (Edwards, NY) was operated for chrome deposition. Tegal Asher (CollabRx, San Francisco, CA) was used for glass surface activation. A spin coater (P-6708, Specialty Coating Systems, Indianapolis, IN) was used to spin-coat photoresist AZ 4330 and KMPR® 1025 on the fused silica wafers. Hotplate (Model 1000-

1, Electronic Micro Systems Ltd., Wiltshire) was used to thermally cure the photoresist film. UV exposure process for patterning photoresist was accomplished by OAI 808 aligner (OAI, San Jose, CA). DISCO Automation Dicing Saw (DAD 3220, Santa Clara, CA) was used to dice fused silica wafers to 13 x 13 mm chips as the substrate for sensor patterning. The photo-patterning of the polymerizable sensors mixed with photoinitiator at 435 nm wavelength was performed by Maskless Photolithography System (SF-100, Intelligent Micro patterning LLC, St. Petersburg, FL). Dektak 150 stylus contact profiler (Veeco, Plainview, NY) was used to measure the thickness of microwells and sensor spots. The optical microscope (LV150, Nikon, Melville, NY), equipped with a digital QIClick CCD camera (Model QIClick-F-M-12, Qimaging, Surrey, BC), was used to image the micro-patterns and measure the dimensions. Eclipse TE2000E Nikon confocal fluorescence microscope (Melville, NY) was used to visualize the fluorescence features of photo-patterned sensors. RF-5301PC spectrofluorophotometer (Shimadzu Scientific Instruments, Columbia, MD) was used for the characterization of the optical sensors.

2.2.2 Micromachining Techniques and Process Flow of KMPR Microwells

The typical fabrication and improved fabrication procedures of backside exposure are compared in **Figure 3** and **Figure 4**. The former (**Figure 3**) reflects a standard photolithography process including spinning KMPR at target speed, UV exposure, and wet etch by MF-26Ato develop micropatterns. As mentioned above, to improve adhesion between KMPR and glass surface, the backside exposure process is applied and demonstrated in **Figure 4**. A 100 nm thin film of chrome was firstly vapor-deposited on the surface of the fused silica wafer. After patterning a 3 μm film of positive photoresist

AZ 4330 on the chrome layer, chrome etchant transferred the same patterns to the chrome layer because of using the photoresist AZ 4330 as a masking layer. A 20 µm KMPR® 1025 was spin-coated on the same side with chrome patterns at 3800 rpm, followed by a soft-bake at 65 ºC for 1 min and at 95 ºC for 5 min on the programmed hotplate with the temperature ramp rate of 1 ºC per minute. UV exposure was carried out with a dose of 485 mJ/cm^2 through the backside with a long pass filter to improve I-line intensity delivered to the resist, and a post-exposure bake was then performed using procedure identical to the soft-bake process. The KMPR film was developed and patterned in the MF-26A developer solution for 5-7 min and then hard baked at 150 ºC for 30 min to remove all the remaining solvent. After the chrome etchant eliminated the residual chrome left on the substrate, the wafer was diced into 13 x 13 mm chips each containing a 3 x 3 array of the KMPR microwells at the center.

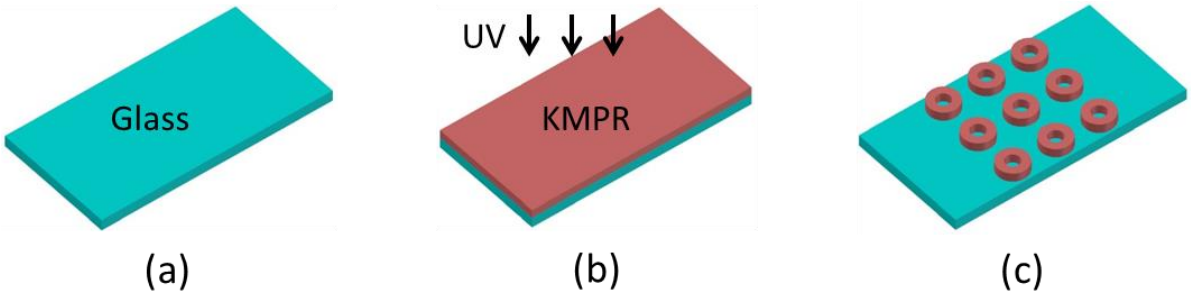

Figure 3. Typical Photolithography Process for KMRP Patterning (Not Scaled). (a) RCA Cleaning, (b) KMPR Spin-Coating and UV Exposure, and (c) KMPR Patterns Developing.

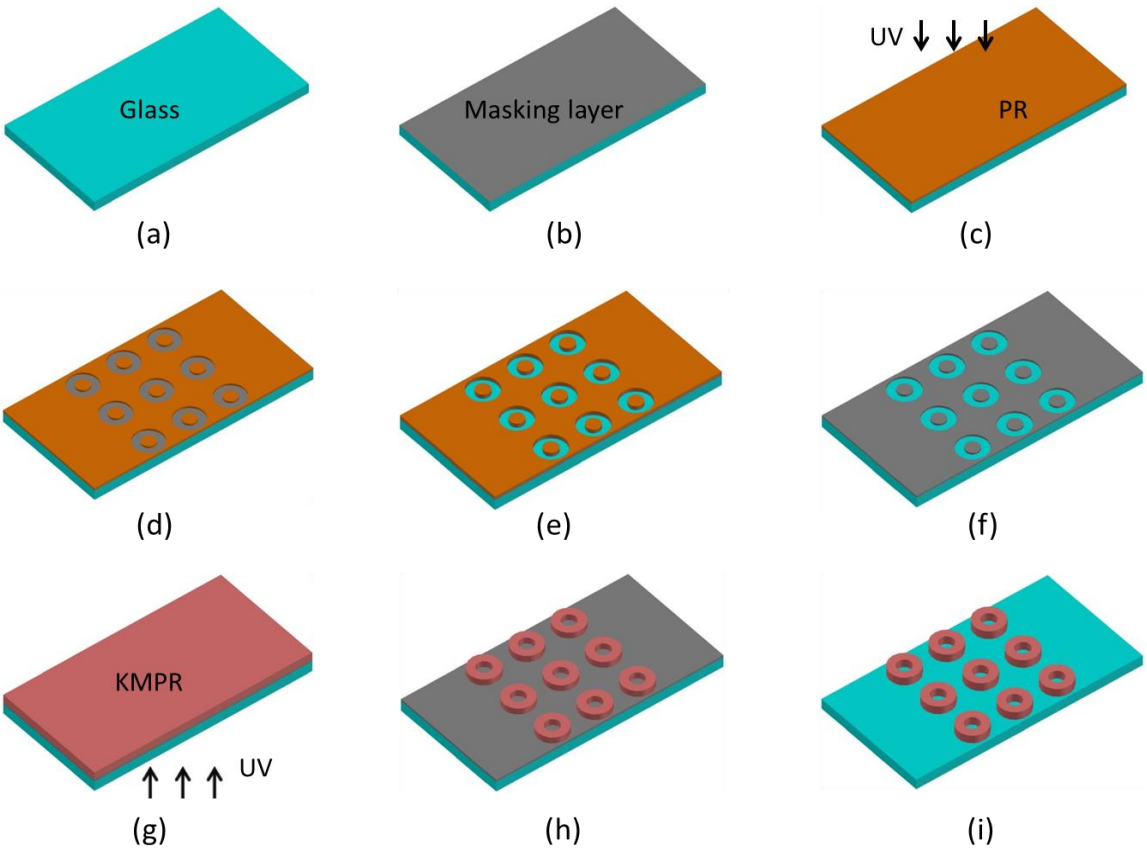

Figure 4. Backside Exposure Fabrication Process Flow of A 3 x 3 Microwell Array (Not to Scale). (a) RCA Wafer Clean, (b) Masking Layer (Chrome) Deposition, (c) Photoresist Spin-Coating and UV Exposure, (d) Photoresist Developing, (e) Masking Layer Etching, (f) Photoresist Stripping, (g) KMPR Spin-Coating and UV Exposure from the Backside, (h) KMPR Developing, and (i) Masking Layer Removal.

2.2.3 Single-cell Metabolic Profiling

2.2.3.1 Photo-patterning of Tricolor Optical Sensor

Comparing to the polymerization of the optical sensors using thermal curing techniques, the photo-polymerizable sensors show a notable advantage in terms of sensor patterning. For thermal polymerization of the optical sensors, a step of plasma etch with masking layers is introduced to pattern the thermal cured sensors (Zhu, Zhou et al. 2012). However, this harsh plasma not only impacts the stability and reliability of the sensors, but also

increases the overall complexity of the procedure. Since photo-polymerizable sensor can polymerize when exposed to UV light, the photo-patterning of the tricolor sensors can be easily performed by using the SF-100 Maskless Photolithography System (MPS), which enables to project a virtual mask and UV exposure onto the substrate surface. Firstly, the surface of fused silica dies were activated by oxygen plasma and functionalized with 3-acryloxypropyl trimethoxysilane. Then a uniform thin film of tricolor sensor solution was applied on the surface through a cover slip silanized by TMSPA. The tricolor sensor was then UV exposed and polymerized at 435 nm wavelength under the designed virtual masks loaded into the system. Methanol could remove the unexposed sensor left on the substrate and eventually sensor patterns with a 300 μm pitch remained on the surface.

2.2.3.2 Cell Loading and Sensor Fluorescence Monitoring

According to the configuration described in **Figure 1**, the fused silica die with the tricolor sensor array is aligned and sealed to the bottom KMPR microwell array (300 μm pitch) loaded with single cells. The KMPR microwells were fabricated containing lips for confinement of single cells using the backside exposure method. CP-A cells, the immortalized human esophageal epithelial cell line, derived from Barrett's Esophagus (a premalignant condition that predisposes to the development of esophageal adenocarcinoma) (Hameeteman, Tytgat et al. 1989) were loaded into the microwells using a cell loader with a home-built piezo-driven pico-pump (Anis, Houkal et al. 2011). After the single cells were incubated for 24 hours, the metabolic "draw-down" assay was carried out on a home-built setup built around an inverted microscope, creating a hermetically sealed microchamber by aligning and sealing the fused silica lid with tricolor sensor arrays to the microwell

arrays. When single cells were hermetically isolated inside the microchamber, the fluorescence intensity of the sensor arrays were automatically collected for 60 min at 1 min interval**Error! Reference source not found.**. The feature of the tricolor sensors provided heterogeneous oxygen and pH responses which can be simultaneously detected from different single cells, while the reference probe showed no response, which could be used as reference in ratiometric analysis. When a set of the oxygen and pH responses were obtained, they were analyzed to calculate ECAR and OCR.

2.3 Results and Discussion

2.3.1 Tricolor Sensor Characterization

Figure 5 shows the pH and oxygen responses of the dual pH and oxygen sensor in PBS buffers. The sensor comprises a pH probe with an emission maximum at 515 nm, an oxygen probe with an emission maximum at 650 nm and an internal built-in reference probe with an emission maximum at 580 nm. **Figure 5** (a) shows the pH responses of the dual sensor when excited at 488 nm. The emission at both 515 nm and 580 nm increase with the increase of pH. This is due to a slight overlay of the fluorescence from the pH probes with the built-in reference probes. When excited at 540 nm, the emission at 580 nm has no response to pH (**Figure 5** (b)). The oxygen sensor with an emission maximum at 650 nm does not respond to pH when excited at either 488 nm or 540 nm. **Figure 5** (c) shows the pH responses of the sensor calculated by the changes of the intensities at 515 nm and also the ratiometric approach using the ratios of emission intensities at 515 nm and at 580 nm. The pH responses cover the physiological ranges from 7.5 to 5.5, indicating its applicability for biological pH measurements.

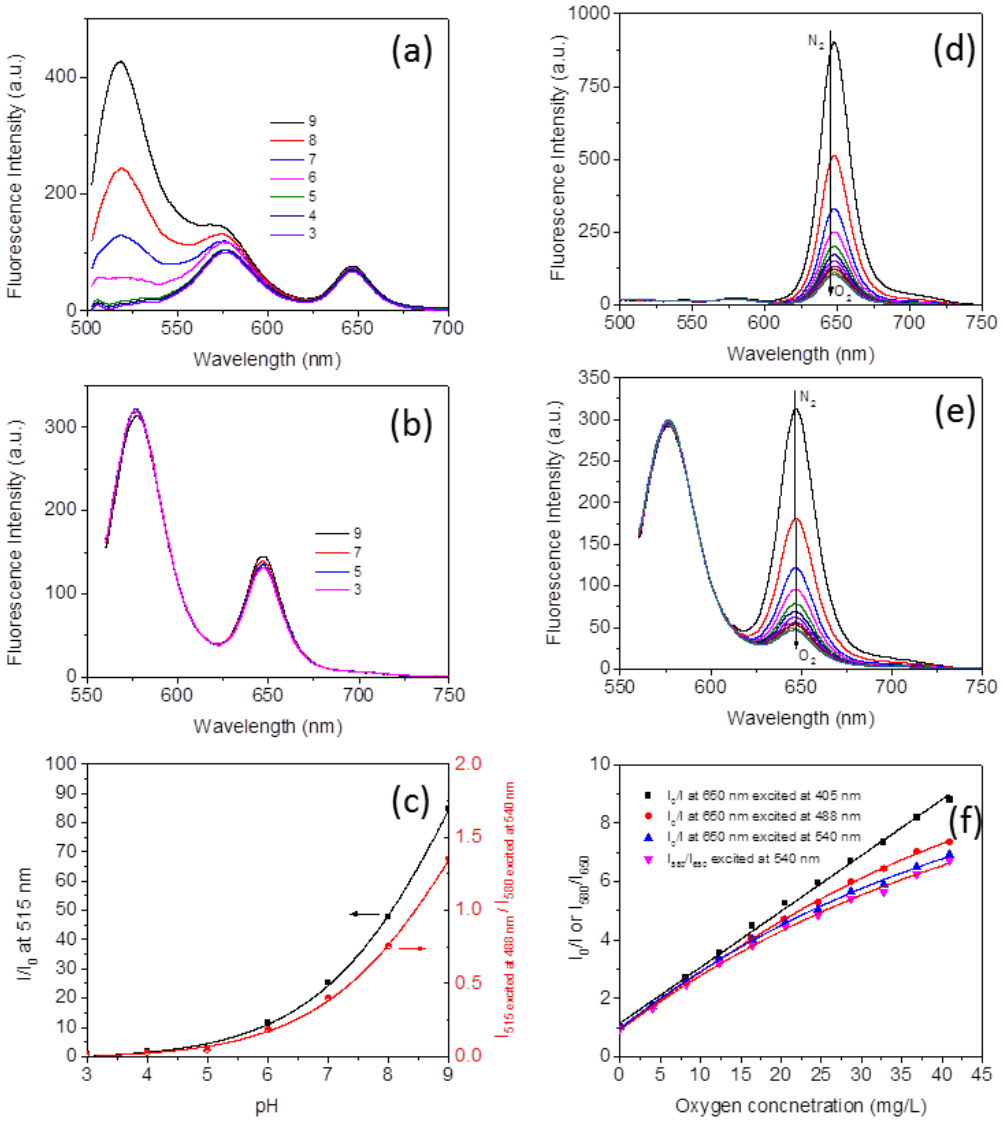

Figure 5. (a) pH Responses Excited at 488 nm; (b) pH Responses of the Reference Probes and Oxygen Probes; (c) pH Responses as Measured Using Emission Intensity at 515 nm and the Ratio between Intensities at 515 nm and 580 nm; (d) Oxygen Responses Excited at 405 nm; (e) Oxygen Responses Excited at 540 nm; (f) Stern-Volmer Plots of the Oxygen Responses Using the Different Methods. Note Dissolved Oxygen in Air-saturated Water at 23 °C is 8.6 mg/L or 8.6 ppm. (Tian, Wang et al. 2016)

Figure 5 (d) and (e) show the oxygen responses excited at 405 nm and 540 nm, respectively. The emission intensities of the oxygen sensor increase with a decrease in dissolved oxygen concentrations, similar to other oxygen sensors. **Figure 5** (f) shows the Stern-Volmer plots

of the oxygen responses calculated using different approaches. The sensor responds linearly to oxygen when excited at 405 nm, because at such an excitation wavelength, the rhodamine derived built-in reference and pH probe were not excited efficiently. Although non-linear Stern-Volmer plots were observed when excited at other wavelengths, such as 488 and 514 nm at high oxygen concentrations, because of the slight overlay of the emissions of the built-in reference probes with the oxygen sensor's emissions, all the plots show linear responses to oxygen from deoxygenated condition to dissolved oxygen concentration of 10 mg/mL corresponding to oxygen fraction of 24% in air. The linear responses make the calculation of oxygen concentrations simple when used for cellular oxygen respiration studies (Tian, Wang et al. 2016).

Considering the KMPR microwell array having an inner diameter of 80 μm, the sensor spots confined to the microwells are designed to have the diameter of 60 μm. When a tricolor sensor array was formed using the MPS, its fluorescence spectrum was analyzed using the spectrum scanning function of the Nikon confocal microscope (**Figure 6**). In **Figure 6** (a), the yellow represents reference sensor reflected an emission maximum at 651 nm when excited at 580 nm; the red represents oxygen sensor imaged at its emission maximum of 650 nm when excited at 405 nm; the green represents pH sensor imaged at its emission maximum of 525 nm when excited at 488 nm. The fluorescence spectrum (**Figure 6**(b)) is similar to the spectrum in **Figure 5**, which suggests minimal photo damage to pH, oxygen and reference sensors during the photo-patterning process.

(a)

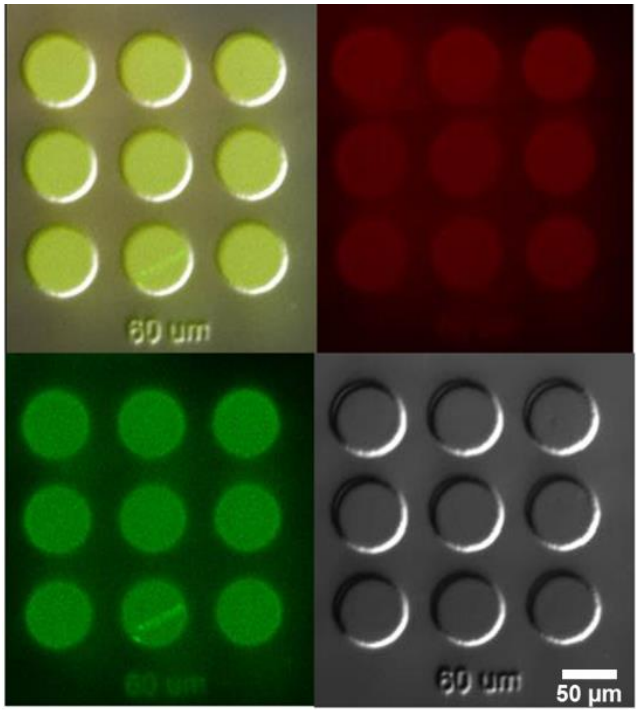

(b)

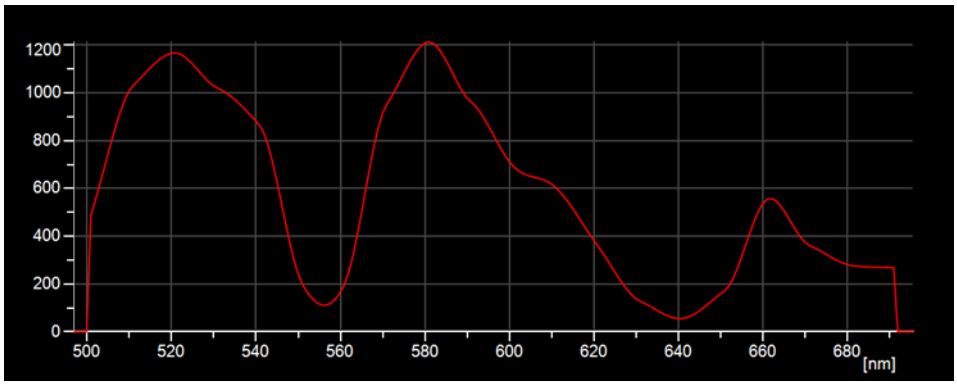

Figure 6. (a) Fluorescence Images and Bright Field Image fom Tri-Color Sensor Arrays Photopolymerized; (b) Fluorescence Spectrum from Fluorescence Image Series in (a).

2.3.2 KMPR Microwells Characterization

Since live cells can be well cultivated on the glass surface (Kelbauskas, Ashili et al. 2012, Kelbauskas, Ashili et al. 2017, Kelbauskas, Glenn et al. 2017), the bottom of the

microwells should only have glass surface after KMPR micro-fabrication process (**Figure 7**). Unlike the unexpected potential result during insufficient wet-develop of standard photolithography procedure causing a thin layer of KMPR still left on the glass surface, backside exposure process can ensure KMPR microwells consisting of clear glass surface if the chrome layer is completely removed. After the microwells were fabricated, the moisture resistance in the cell culture medium was tested. Considering the single cells contained in the KMPR microwells need to be cultivated in the cell culture medium for 24 hours before a 2 hour metabolic profiling, the test of the moisture resistance was designed to last for 72 hours. In **Figure 8** (a), an array of KMPR microwells on a 13 x 13 mm fused silica chip fabricated by the backside exposure method was kept in the cell culture medium for 3 days and the yield of the microwells left on the chip was measured showing a result of no microwells peeled off. In **Figure 8** (b), the KMPR microwells fabricated by the typical photolithography process including UV exposure from the top of KMPR layer through the photomask presented a serious issue that some microwells were peeled off in the same condition.

To display significant responses of the extracellular sensor to the single cells in the microwells within a reasonable time (few minutes to a few hours), the volume of the microwells needs to be considered. Based on the average oxygen consumption rate of single cells measured by others and our team, microwell dimensions were designed similarly to the earlier approach in CBDA (Kelbauskas, Ashili et al. 2012): bottom of 80 μm (inner diameter) and sidewall of 20 μm height, creating a microwell with 100.5 pL volume. It is critical to have the same microchamber volume for calculating the metabolic rate parameters (ECAR and OCR), so the uniformity of the microwell height becomes one

of the most important factors in this fabrication process development. The heights of each microwell in the 3 x 3 array were measured using a contact stylus profiler and the results were plotted in **Figure 9** (the dot position represents well number). The microwells located on one side of the array were slightly higher than those located on the other side of the array. However, the difference was only about 0.1 µm for 20 µm height, resulting in negligible variations (~0.5%) in volume related metabolic measurements.

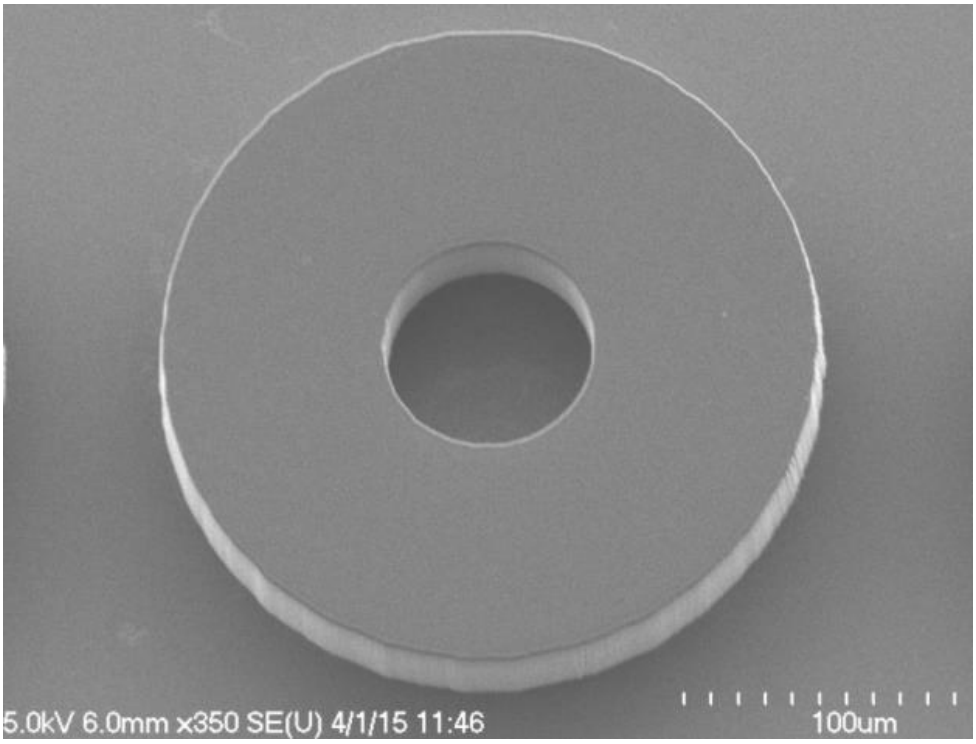

Figure 7. FESEM Image of KMPR Microwell.

(a)

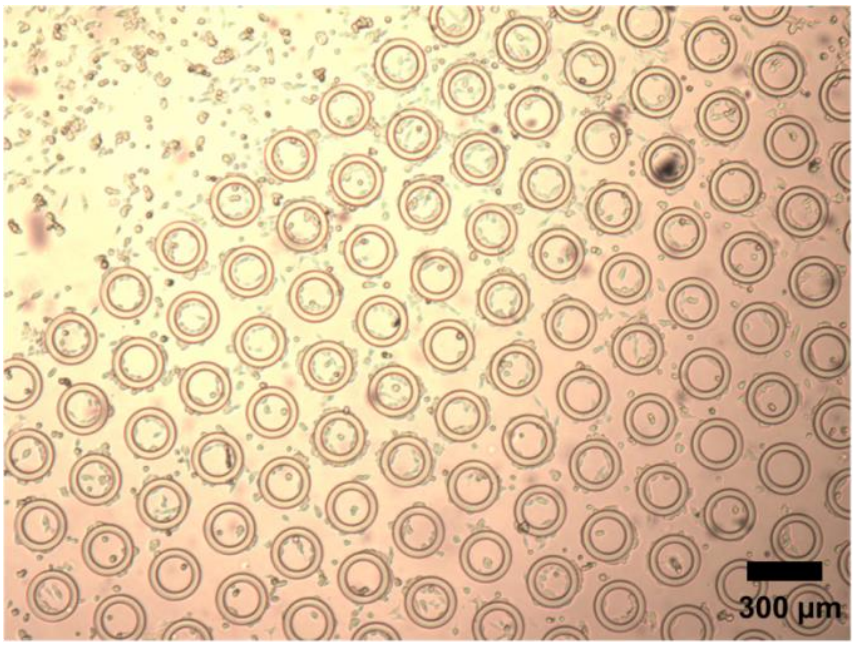

(b)

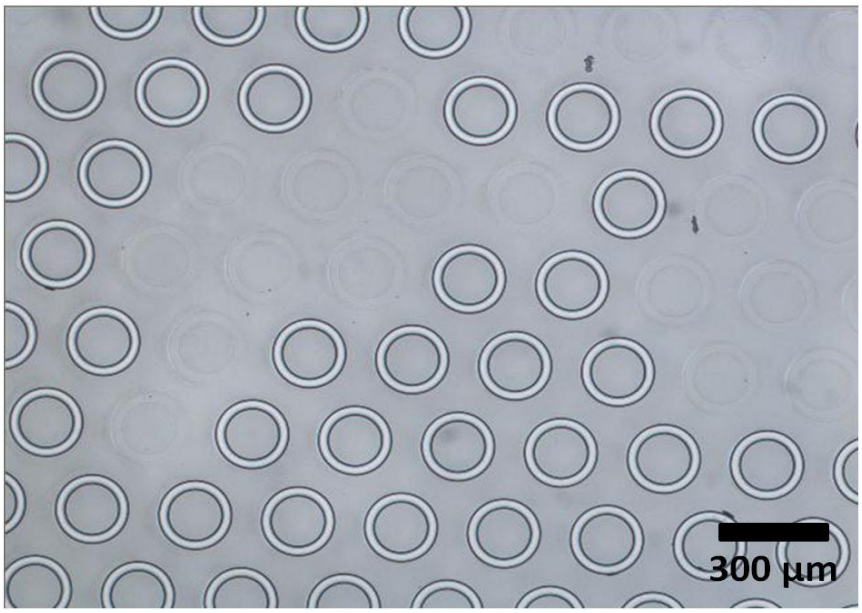

Figure 8. Moisture Resistance of KMPR Microwells in Cell Culture Medium after 72 Hours Fabricated by (a) Backside Exposure Process; (b) Typical Photolithography Process.

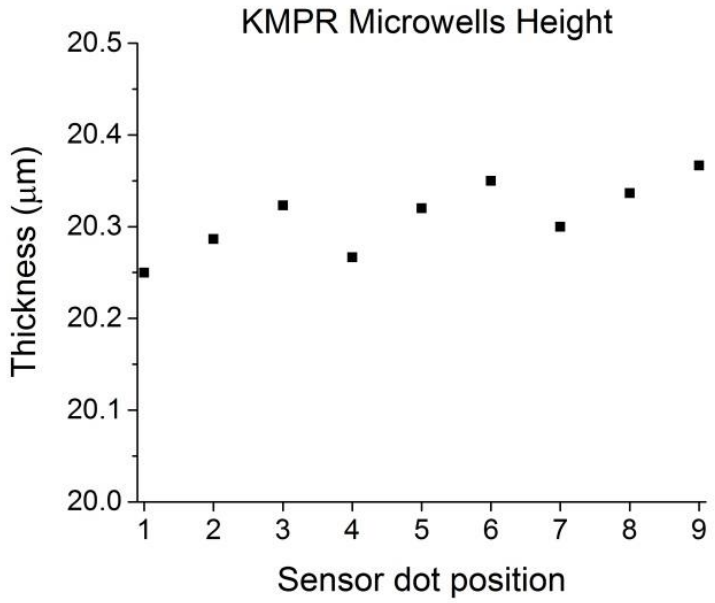

Figure 9. Height of a 3 x 3 KMPR Microwell Array.

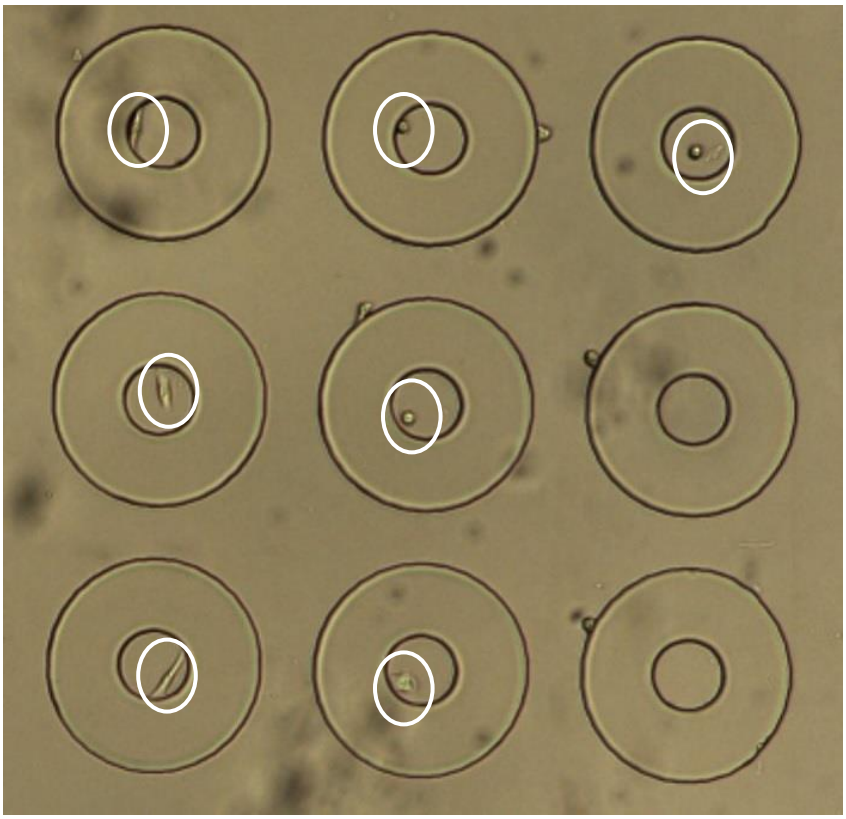

Figure 10. Single Cells Loaded in KMPR Microwells with an 80 µM inner diameter.

2.3.3 Single Cell Metabolic Profiling

The fabricated KMPR microwell arrays were loaded with metaplastic CP-A cells derived from Barrett's Esophagus and incubated for 24 hours (**Figure 10**). Two microwells with no cells were used as control. After the "draw-down" was properly performed by aligning sensor arrays to the microwell arrays, the fluorescence intensities from tricolor sensor arrays were automatically collected for 60 min at 1 minute intervals at 37 ºC. To relate the fluorescence intensities to pH and oxygen concentration, a calibration of oxygen and pH responses of the tricolor sensor was performed using the "draw-down" station. A fused silica substrate (13 mm x 13 mm) was coated with a thin film of the tricolor sensor and immersed in cell culture medium for the fluorescence measurement at 37 ºC. For pH response, pH value of the medium was set from 6.0 to 8.0 with an interval of 0.5. For oxygen response, the oxygen and nitrogen mixtures of different volume ratios were used to purge the medium to set a series of different dissolved oxygen concentrations. When the data collection of the fluorescence intensity corresponding to different conditions described above was completed, the relation between intensity and pH value or oxygen concentration of the cell culture medium was plotted (**Figure 11**). In particular, the pH response follows the sigmoidal function:

$$\frac{I}{I_0} = \frac{m_2 - m_1}{1 + \exp(pK_a - pH)/p} + m_1$$

Where I represents the fluorescence intensity measured at different pH values during the experiment and I_0 represents that at the lowest pH value (pH = 3); m_1, m_2, pKa, and p are,

respectively, the initial value, final value, point of inflection and width of the sigmoid curve. For oxygen response, it follows the linear Stern–Volmer equation:

$$\frac{I_0}{I} = 1 + K_{svq}[O_2]$$

Where K_{svq} is the Stern–Volmer quenching constant and $[O_2]$ is the corresponding dissolved oxygen concentration. I_0 is the steady state fluorescence signals measured at 0% and I represents various dissolved oxygen concentrations. When the fluorescence intensities reflecting the metabolic activities of live single cells in the KMPR microwells were recorded, pH and oxygen kinetics of each single cell were calculated and plotted according to the calibration of the tricolor sensors **(Figure 12**). In **Figure 12** (a), two microwells with no cells reflect that the oxygen concentration didn't change in 60 minutes while other seven single cells exhibited different OCRs in each sealed microwell. In **Figure 12** (b), the pH value in the seven microwells containing the single cells decreased. Particularly, to reveal whether the microwells were successfully sealed, oxyrase, an enzyme that removes dissolved oxygen, was added to the medium outside the microwells and the fluorescence responses of the tri-color sensors inside the microwells were monitored and plotted. The flat curves from the sensor indicated that the oxygen concentration in the sealed microwells was not affected by environment outside the microwells.

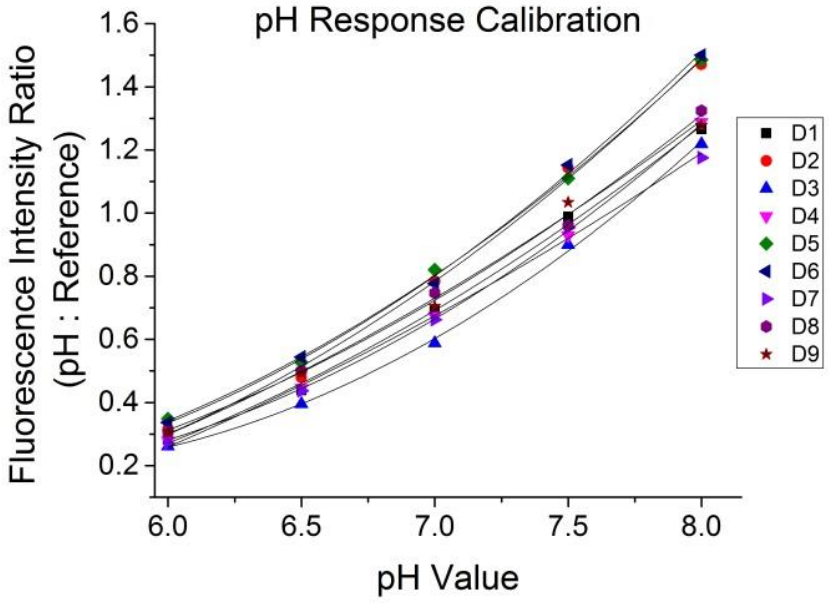

(a)

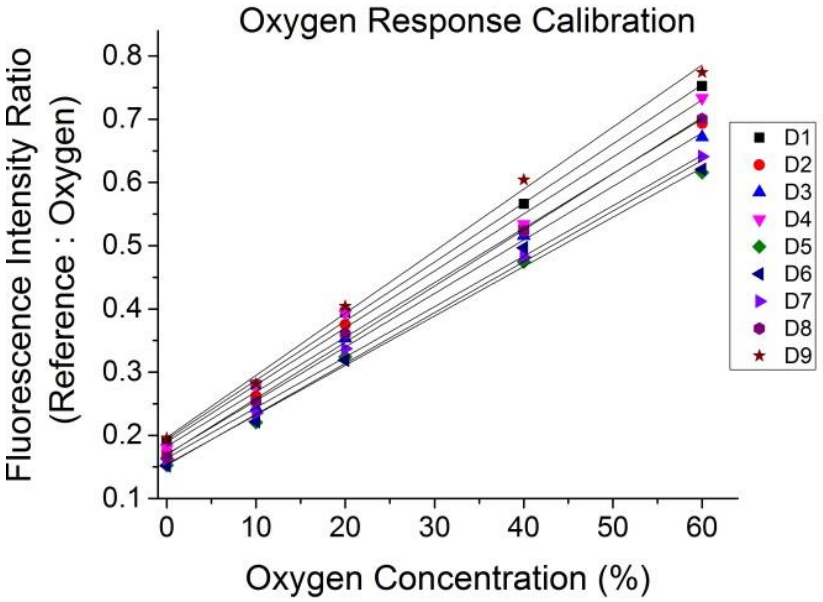

(b)

Figure 11. Characterization of a 3 x 3 Tricolor Sensor Array.

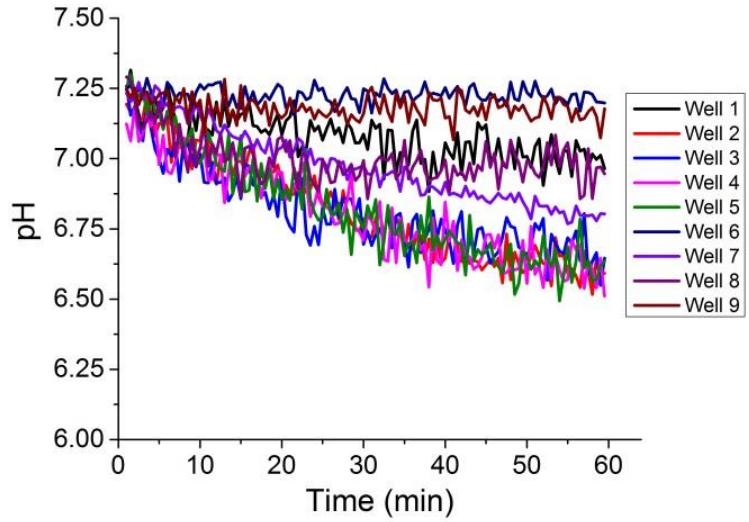
7.50
7.25
7.00
6.75
6.50
6.25
6.00
pH
0
10
20
30
40
50
60
Time (min)
Well 1
Well 2
Well 3
Well 4
Well 5
Well 6
Well 7
Well 8
Well 9

(a)

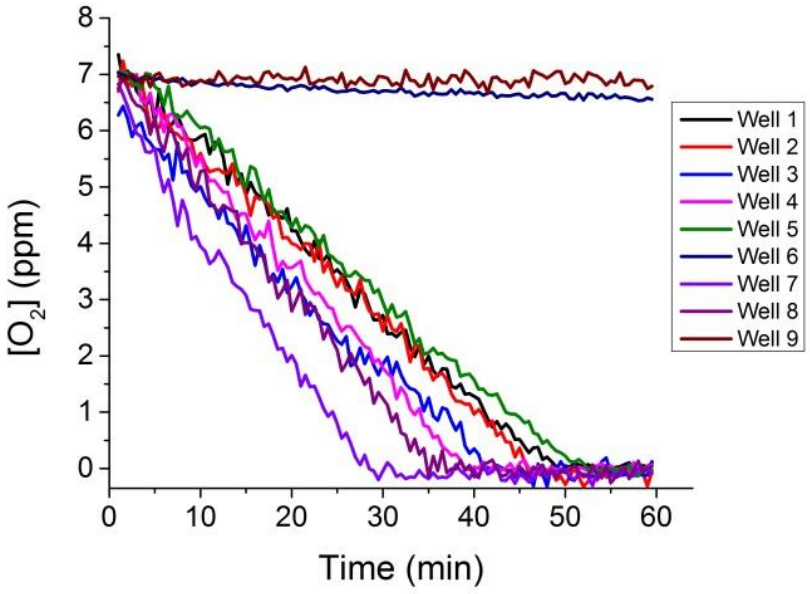
8
7
6
5
4
3
2
1
0
[O2] (ppm)
0
10
20
30
40
50
60
Time (min)
Well 1
Well 2
Well 3
Well 4
Well 5
Well 6
Well 7
Well 8
Well 9

(b)

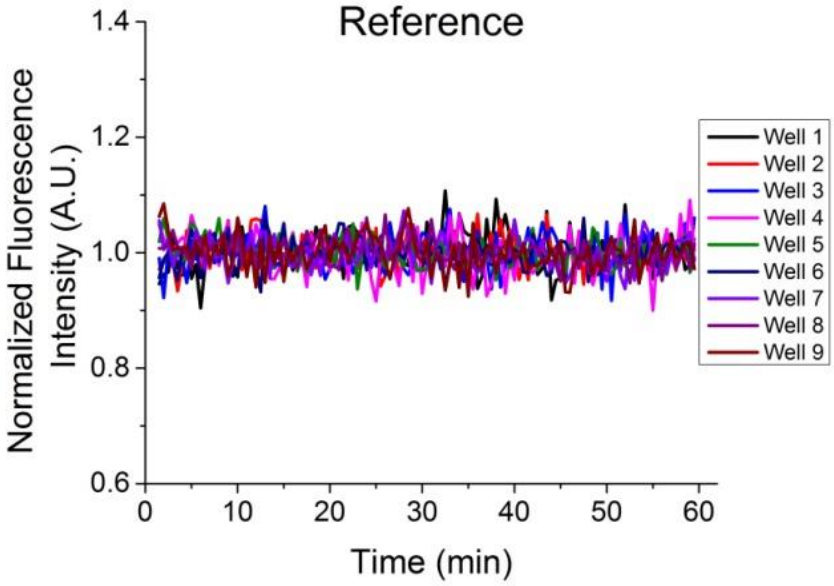

(c)

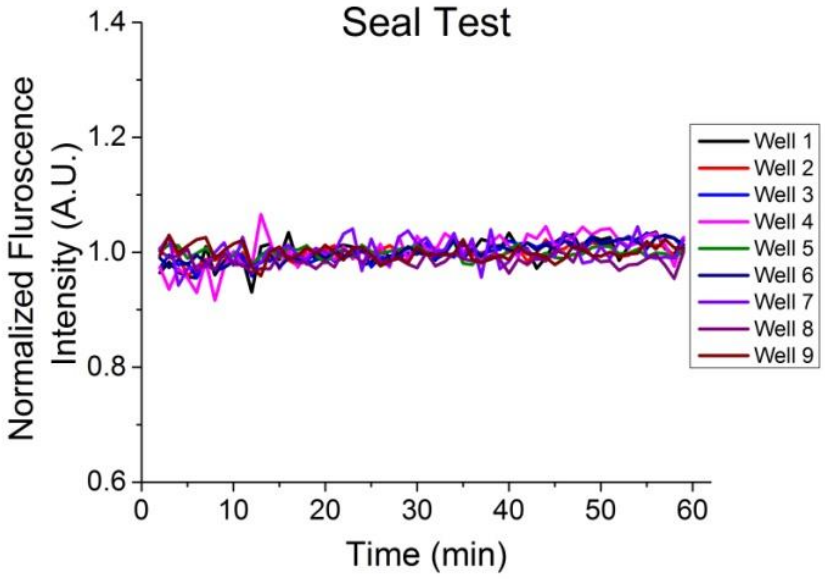

(d)

Figure 12. Single Cell Metabolic Profiling. (a) pH kinetic; (b) Oxygen kinetic; (c) Reference; (d) Seal Test.

2.4 Conclusions

In this work, a backside exposure process for patterning KMPR microwell arrays was successfully developed and O2 and pH kinetics of live single cells with tricolor optical sensors was measured. The process shows a good moisture resistance of KMPR microwells with uniform thickness for single-cell metabolic profiling analysis. The improved method provides a flexible and reliable foundation for high-throughput, multiparameter analysis of live cell respiration and other metabolic parameters at the single-cell, multiple-cell and tissue level.

3. DEVELOPMENT OF A MICROFLUIDIC DEVICE USING OIL SEAL METHOD FOR SINGLE-CELL METABOLIC ANALYSIS

In this Chapter, an optimized microfluidic device is demonstrated for single cell metabolic profiling based on hermetic sealing with oil. SU-8 fabrication and microfluidic techniques were used to assemble 10 × 10 single cells and tri-color sensors, using heavy mineral oil as a sealing material. This approach allows rapid single-cell trapping, multi-parameter cellular metabolic analysis and drug screening.

3.1 Introduction

One major challenge for single-cell analysis is to develop techniques to achieve multi-parameter metabolic analysis. To investigate alterations in the physiologic state of individual cells including their phenotypes and responses to the stimuli in the microenvironments, multiple appropriate parameters need to be measured with high sensitivity and accuracy in single cells (Wu, Neilson et al. 2007). Multi-parameter analysis could provide new perspectives to uncover the mechanism of inter- and intra-cellular interactions (Torres-García, Ashili et al. 2012, Smallwood, Lee et al. 2014). Applications of fluorescent optical sensors bring insights into analyzing multiple cellular metabolic parameters (Zhu, Holl et al. 2009). The advantages of optical sensors in biological applications, compared to the traditional electrochemical probes, are their faster response, higher sensitivity, more simple manipulation, remote sensing capability, and noninvasiveness(Park, Reid et al. 2005, Snijder, Sacher et al. 2009). This is especially beneficial when studying single-cell physiological phenotype, because the in situ detection

on the responses of a very small change of analytes is required. Most importantly, to simultaneously measure multiple parameters, it requires analyzing single cells in a multiplexed fashion (Kelbauskas, Glenn et al. 2017). Fluorescent optical sensor is capable of offering the multiplexing function by spatially separated microsensors (Ray, Zhu et al. 2010), which could be integrated with microfeature arrays (such as microwells) to perform multi-parameter sensing. As a result, sensor patterning in multi-spot array structures is particularly critical. Although an approach to use multiple cycles of deposition, photoresist patterning and oxygen plasma etching on thermal polymerizable sensors has been reported (Zhu, Zhou et al. 2012), the performance of oxygen sensors was compromised due to the harsh plasma treatment conditions. In addition, the microstructure for sensor deposition is quite small (a diameter of around 100 μm and a depth of about 20 μm), and hence it usually requires advanced instrumentation to deposit a small volume (around 100 to 200 pL) of the sensor precursors. In this paper, a photo-patternable dual pH and oxygen sensor with tri-color emissions was selected because it enables a more convenient, mild and flexible patterning process compared to the plasma etching method.

Another challenge is to improve the technology for the immobilization and separation of single cells. The reported methods (Dragavon, Molter et al. 2008, Molter, Holl et al. 2008, Etzkorn, Wu et al. 2010) are based on random seeding of cells by gravity into surface-modified microwells, but the bottleneck was that it was extremely difficult to precisely control the numbers of single cells per location. To overcome this limitation, a platform using a piezo-driven pico-liter pump to select and transfer individual cells to a 3 × 3 microwell array was demonstrated (Anis, Houkal et al. 2011). However, the time needed for loading cells would increase drastically when larger arrays are used. Microfluidic

hydrodynamic traps can immobilize cells in narrow gaps since cells are too large to pass through (Wheeler, Throndset et al. 2003). Multiple hydrodynamic traps are fabricated and positioned at particular distance inside microfluidic channels, and cells are directed into the traps by on-chip valves that can perform high precision control of fluid flow. The dimensions can be designed to draw only one cell for each trap, and once one trap is filled, other cells will move forward to next traps. This trapping mechanism allow hundreds of single cells to be retained individually by a large hydrodynamic trap array in a relatively short time period.

In this chapter, an improved and efficient microfluidic platform for single-cell metabolic profiling analysis including measurements of oxygen consumption rate and pH changes in the cellular microenvironment is reported. The system is based on a microfluidic device containing extracellular fluorescent optical sensors to perform multi-parameter metabolic phenotype characterization in single cells. The approach utilizes a hydrodynamic method for immobilizing individual cells in particular arrangement with convenience, rapidness and high precision. The layer with the trapped cells is aligned and assembled with a microwell array confining optical sensors, which is enclosed by mineral oil for hermetically sealing. In addition, the design of the configuration allows medium exchange by automated syringe pump, which provides a fundamental basis for drug screening on the same cell.

3.2 Materials and Methods

3.2.1 Materials and Reagents

Four inch double side polished fused silica wafers (University Wafer, South Boston, MA) of 500 μm thickness were used as the substrate. RCA 1 clean and RCA 2 clean were

processed by a mixture of 1 part of 27 wt% ammonium hydroxide, 1 part of 30 wt% hydrogen peroxide and 5 parts of DI water, and a mixture of 1 part of 35 wt% hydrochloric acid, 1 part of 30 wt% hydrogen peroxide and 5 parts of DI water, respectively. AZ4330 positive photoresists, AZ300 MIF developer, chromium source and chromium etchants (mixtures of perchloric acid and ceric ammonium nitrate) were provided by the Center for Solid State Electronics Research (CSSER) (Arizona State University, Tempe, AZ). Photoresist SU-8® 3025 and SU-8 Developer were purchased from Microchem Corp (Westborough, MA) to fabricate microfluidic channels and microwells by photolithography. Trimethylsilylpropyl acrylate (TMSPA), (Tridecafluoro-1,1,2,2-tetrahydrooctyl)-1-trichlorosilane, carbonyl cyanide 3-chlorophenylhydrazone (CCCP) Dimethyl sulfoxide (DMSO), and heavy mineral oil were commercially available from Sigma–Aldrich (St. Louis, MO). A photo-polymerizable tricolor sensor (pH probe, oxygen-probe and reference-probe) was synthesized by the chemistry group led by Dr. Yanqing Tian in CBDA (Arizona State University, Biodesign Institute) (Tian, Wang et al. 2016). PDMS (Sylgard 184, Dow Corning) was polymerized and used as planar compliant layers. Polymethylmethacrylate (PMMA) sheets (Goodfellow, Coraopolis, PA) were precisely micromachined by laser to connect fabricated chips with microfluidic ports and tubing. LIVE/DEAD® Cell Imaging Kit (488/570) was acquired from ThermoFisher Scientific (Waltham, MA) for cell viability.

3.2.2 Instruments

Tegal Asher (CollabRx, San Francisco, CA) was utilized for glass surface activation. Edwards Auto 306 E-beam Evaporator (Edwards, NY) was used for chromium deposition.

A spin coater (P-6708, Specialty Coating Systems, Indianapolis, IN) was used to spin coat photoresist on the fused silica wafers. A hotplate (Model 1000-1, Electronic Micro Systems Ltd., Wiltshire) was used to bake the resist film. OAI 808 aligner (OAI, San Jose, CA) were used for UV exposure to form SU-8 microstructures and polymerized sensor patterns. Dektak 150 stylus contact profiler (Veeco, Plainview, NY) was used to measure the thickness of microwells and sensor spots. DISCO Automation Dicing Saw (DAD 3220, Santa Clara, CA) was used to dice fused silica wafers into 16 x 12 mm chips as the substrate for cell loading and sensor deposition. Eclipse TE2000E Nikon confocal fluorescence microscope (Melville, NY) was used for imaging stained live cells and recording fluorescent intensities of optical sensors. XL-9200 Laser Engraving and Cutting System (Universal Laser Systems, Scottsdale, AZ) was used to form particular patterns on PMMA and PDMS layers.

3.2.3 Configuration Design and Improved Process Flow

The approach is based on forming hermetically sealed microchambers by heavy mineral oil of about 80 pL volume, containing single cells and extracellular fluorescent optical sensors embedded in a polymeric matrix (**Figure 13**) and was previously invented and conceptualized in CBDA (Rodrigues, 2014). To quantify the alterations of microenvironmental oxygen concentration and pH value of single cells, a ratiometric approach was used to measure the ratios of sensor emission intensities through optical sensing equipment for getting accurate analytical data in the sealed microchambers. In the current implementation, the configuration consists of two glass chips both fabricated with symmetrically arranged SU-8 microstructures, one patterned with 10 × 10 microwells (70

μm ID, 120 μm OD and 20 μm deep) and one patterned with 10 × 10 cell traps (21 μm deep) in 10 microfluidic channels as shown in **Figure 14**. When the two chips were aligned and assembled using the four alignment marks at the corners, the heavy mineral oil was introduced into the channels to completely displace the aqueous medium on the outside of the microchambers as a sealing material. The optical sensor fluorescence intensities were extracted to measure oxygen and pH concentration. Particularly, the height difference between the two chips created a 1 μm gap, which allowed a second medium (mixed with a drug) to rapidly displace the oil and enter the microchambers without separating the two chips for monitoring the response of the same cells to the drug.

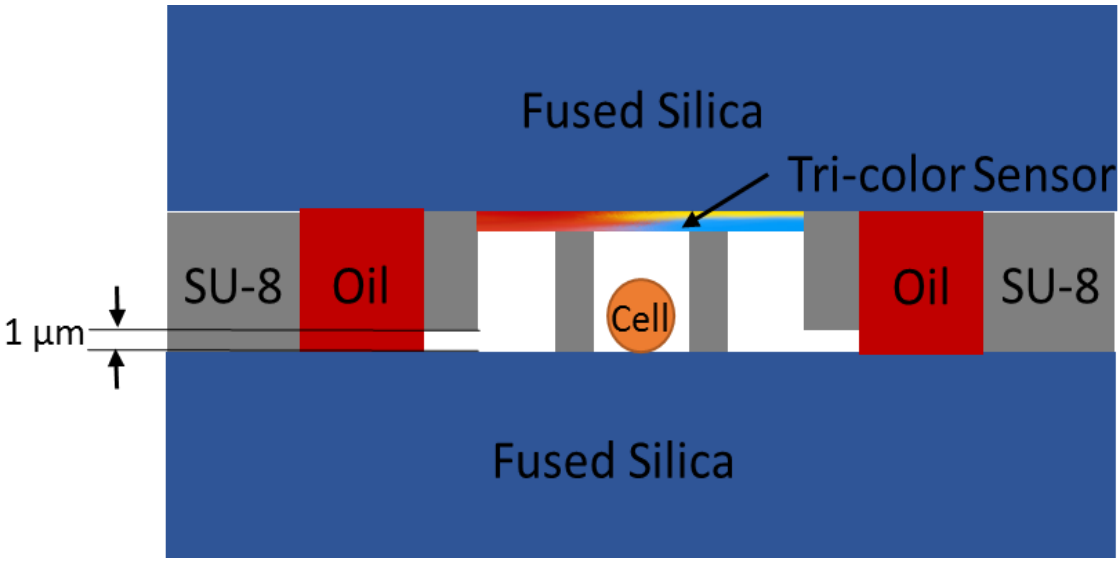

Figure 13. Oil-based Sealing Method Configuration.

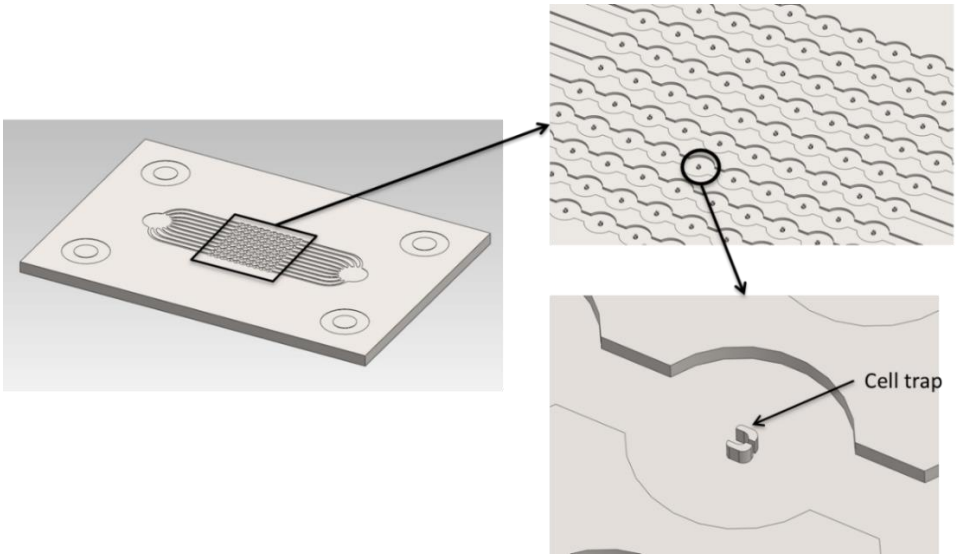

(a)

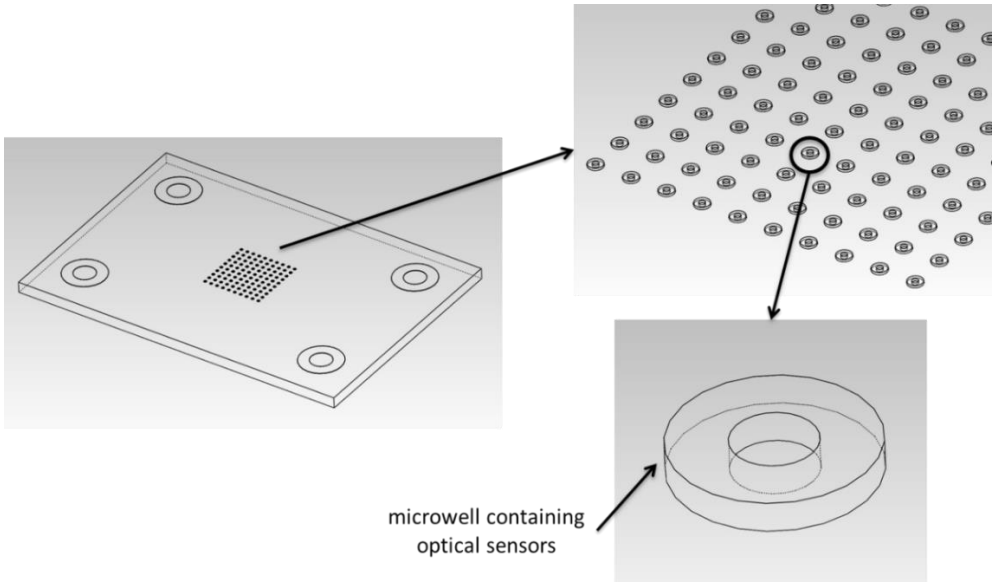

(b)

Figure 14. Microstructure Array Design and Characterization. (a) Design of a 10 × 10 Cell Traps on a 16 mm × 11 mm, 500 µM Thick Fused Silica Die; the Length of Each Channel is 10 mm and Width is 100 µM; Dimension of the Opening of The Trap is 18 µM and the Smallest Gap is below 5 µM. (b) Design of a 10 × 10 Microwell Array on a 16 mm × 11 mm Fused Silica Die of 500 µM Thick Which Can Be Aligned to the Trap Array. (**Figure 14** Courtesy of Wacey Teller.)

To achieve better adhesion between the glass surface and SU-8 patterns, the backside exposure process described in Chapter 2 was applied to the two chips, which resulted in high tolerance to a long time immersion in medium for SU-8 structures without delamination. The original fabrication procedures and improved fabrication procedures are compared in **Table 1**.

Table 1: Detailed Process Flow of The Original Frontside and Optimized Backside Exposure

Important steps	Original front-side exposure	Optimized backside exposure
Wafer preparation	RCA cleaning Dehydrate at 160° C for 30 minutes Surface treatment by oxygen plasma for 10 minutes at 200 W and 300 mTorr	Same
Patterned chrome layer	Not applied	100 nm Cr coating Spin speed 4500 rpm (40 seconds) for AZ 4330 Softbake: 90 seconds Exposure: 150 mJ/cm^2 AZ300MIF development Develop about 90

		• Rinse in DI water and dry with Nitrogen blows • Patterns inspection • Hardbake 110°C for 3 minutes • Chrome etch for about 2 minutes • AZ 4330 removal by Microstrip
SU-8 patterning	SU8 3025: • Spincoat: 4000 rpm for 20 µm thickness • Softbake: 1 minute at 65° C and then an infinity (>5° C/minute) ramp to 95° C and hold for 10 minutes on a hot plate; cool to room temperature (R.T.) • Exposure: 225 mJ/cm^2 with and i-line filter • Post Exposure Bake: Ramp at infinity to 95 °C from R.T.	SU8 3025: • Spin speed 4000 rpm for 20 µm thickness on chrome side • Softbake: Ramp from R.T. to 95° C and hold for 5 minutes; remove from hot plate until cooling to R.T. All ramps, applied for softbake, post exposure bake and hardbake, were set to 1°C/minute • Exposure: 225 mJ/cm^2 with and i-line filter. The SU8 (chrome) side faced down on the OAI aligner stage • Post Exposure Bake: Ramp at 1°C/minute to 95 °C from R.T.; cool to R.T. at 1°C/minute

	• Develop for 4-5 minutes with agitation and inspection • Hardbake: Ramp at infinity to 150 °C.	• Develop for 4-5 minutes with agitation and inspection • Hardbake: Ramp at infinity to 150 °C from R.T.; cool to R.T. at 1°C/minute
Chrome etch	Not applied	• Chrome etch for about 2 minutes

3.2.4 Mineral Oil as a Sealing Material

Previous works reported using mineral oil as a sealant ,(Howland and Bernstein 1931, Alderman, Hynes et al. 2004, Diepart, Verrax et al. 2010, Koivula, Jalkanen et al. 2016) based on one of the most important features of mineral oil, which has much lower diffusion rate of oxygen compared with water (Dumont and Delmas 2003) This property enables mineral oil to be utilized to isolate the individual cells and cell culture media contained in the microchambers from external microenvironment. Furthermore, the spreading coefficient (S) and the interfacial tension (γ) between oil and water surface allow that oil can fully displace an aqueous cell culture media on a SU-8 surface when introduced into microfluidic channel which has been filled with cell culture media.(Zettlemoyer, Aronson et al. 1970, Fay 1971) These characteristics theoretically prove that mineral oil can be used as a soft sealing material integrated with microfluidic devices.

3.2.5 Cell Loading into Microtraps

For this study, one human alveolar adenocarcinoma epithelial cells (the A549 cell line) was used. Millions of A549 cells were cultured to approximately 80% confluence in T-25 tissue-culture flasks (Corning, Corning, NY) at 37 ºC and 5% CO2 atmosphere, and then trypsinized for 5 minutes, followed by a centrifugation at 900 rpm for 4 minutes and re-suspension of approximate 100,000 A549 cells in 3 mL of cell growth medium. Finally, the cells were filtered to single cells by a cell strainer (Corning, Corning, NY) and the single cells solution was prepared in a 3 mL syringe (Thermo Fisher Scientific, Waltham, MA) for cell loading.

To execute rapid cell loading on the 10 × 10 trap array, a 16 mm × 11 mm fused silica chip was sandwiched between two PMMA patterned layers (bottom layer had a compliance PDMS film) as shown in **Figure 15**. When cell suspension was introduced into the microfluidic channels through the inlet, the cells are immobilized in the traps by the fluid flow. In practice, considering some unpredictable tiny debris existing in the fluid which could block the traps, it is desirable to have a single cell occupancy rate after cell loading to be above 95% as a qualified result to proceed by using transmission bright-field imaging. When a high occupancy of trapped single cells was observed, the chip was moved from the cell loading fixture to fresh cell culture media to allow cells to acquire nutrients and oxygen, and then they were cultivated under normal physiologic conditions for a 24 hour growth. In this period, most of the single cells would adhere to traps, but a handful of cells would migrate to the neighboring area. Therefore, it is desirable to achieve an occupancy rate of more than 90% after 24 hour incubation to be used in the assembly. When the occupancy rate is lower than 80%, the cell loading process is started over on a new chip since the average rate was counted to be around 85% to 90% with optimized cell loading method

(double centrifugation and immediate incubation in fresh cell culture media). Cell viability after cell incubation using LIVE/DEAD® Cell Imaging Kit (488/570) (ThermoFisher Scientific, Waltham, MA) was assessed on a confocal fluorescence microscope, at which the cell health and enzymatic activity were reflected by the fluorescent responses. Since cell death of the single cells could happen before or after cell loading, it is acceptable at most 5% dead cells left on the cell traps for experiments. Particularly, occasional cell division occurred during incubation time, indicating a healthy status and near-normal function after confinement in cell traps, but they were not included in the data analysis.

(a)

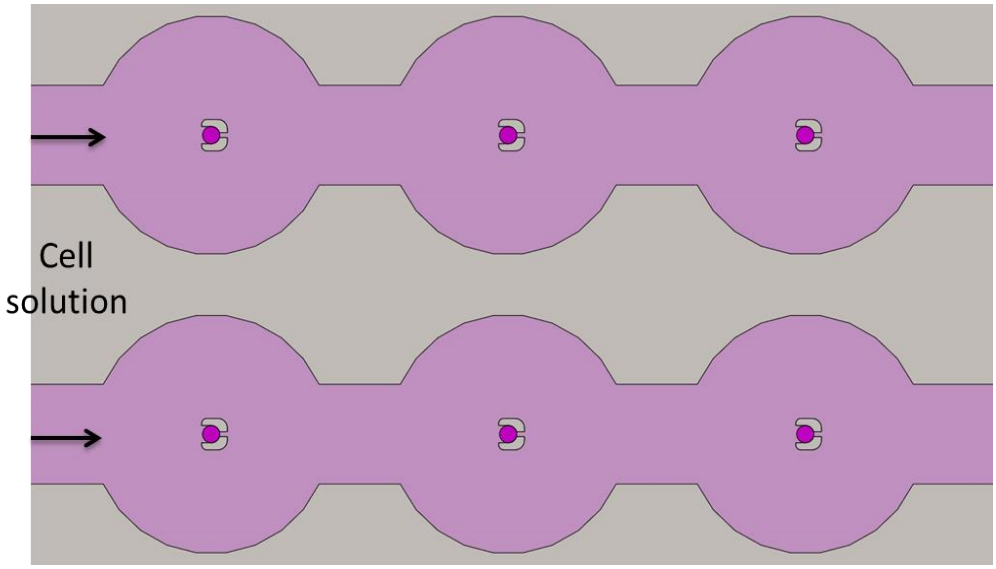

(b)

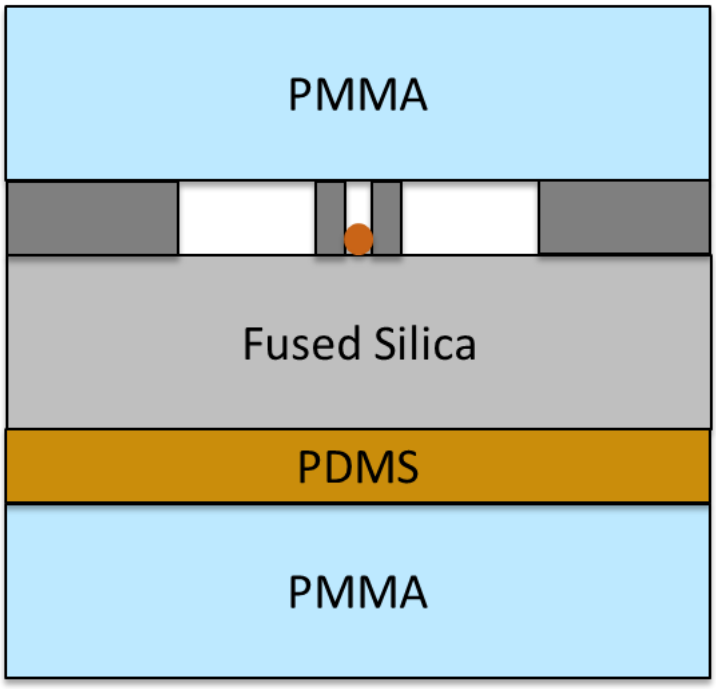

(c)

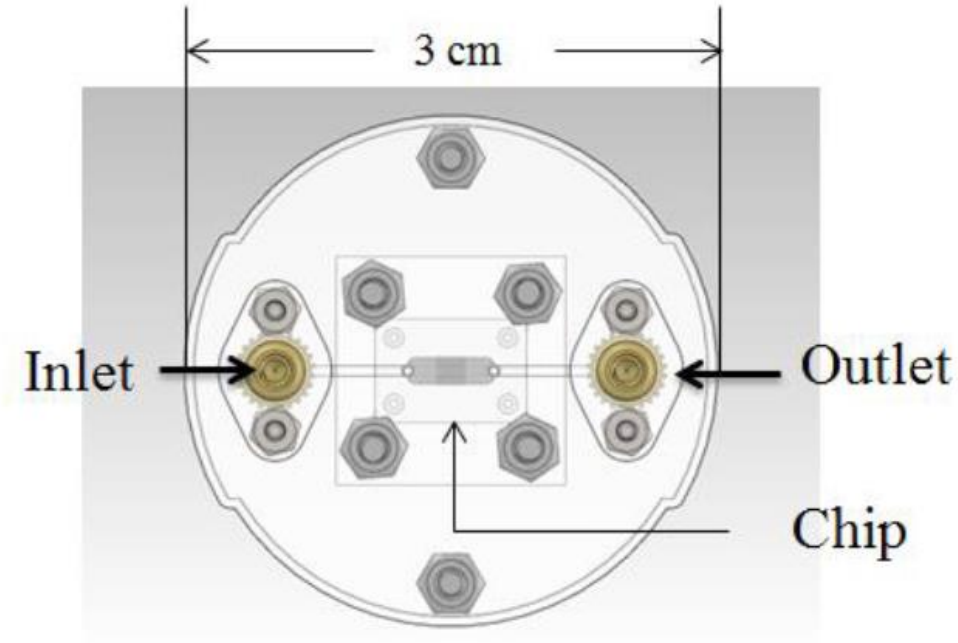

(Rodrigues, Meldrum et al.)

Figure 15. A549 Single Cell Loading Process and Fixture.

3.2.6 Sensor Deposition

As reported previously (Zhu, Zhou et al. 2012), thermal polymerizable sensor into single-cell analysis devices was deposited, using multiple cycles of deposition, photoresist patterning and oxygen plasma etching. In this design, thermal polymerizable sensors were firstly applied by tightly sandwiching microwells and 1 μL sensor solution between two planar glass lids, and then using sonicator to remove extra sensors at the interstitial area among microwells. After an 18 hour curing in an 80 ºC oven and 100% nitrogen atmosphere, the optical sensors were polymerized inside the 10 × 10 microwells. However, the shortcoming of this method is the difficulty of controlling the sensor thickness. As shown in **Figure 16**, the thickness of the deposited sensor in the microwells could reach up to 10 μm while the height of the microwell was around 20 μm, which would generate a much larger gap than 1 μm when the microwells were constructed to the cell traps and dramatically increase the possibility of mineral oil entering the assembled microchambers.

Photo-patterning provides an alternative procedure to deposit optical sensor arrays in the microwells, as most importantly the thickness is dependent on the UV exposure time applied on the sensor liquid. **Figure 17** shows a developed process to deposit photo-patternable sensors in the microwell. The optical sensor liquid solution was synthesized by the chemical group in CBDA led by Dr. Tian, which is composed of dual pH and oxygen probes and an internal built-in reference probe (no response to pH or oxygen) (Tian, Wang et al. 2016). After the surface of glass chip with patterned SU-8 microwells was modified by TMSPA to enable the sensors to be chemically grafted onto the substrate, 1 μL of sensor was deposited, followed by the placement of a thin piece of glass treated with

perfluorooctyltriethoxysilane to prevent sensor adhesion. When the sensor spread over the entire area (**Figure 17** (b)), an external force (either by an air gun, sonication or filter paper absorption) was applied to remove the sensor material left in the interstitial areas among the microwells (**Figure 17** (c)). Then the filtered UV light irradiated on the sensor for 15 seconds, the glass clip was removed from the polymerized membrane surface. The thickness was measured by a surface contact profiler (DEKTAK 150, Veeco, Plainview, NY) and the sensor responses to changes in oxygen concentration and pH of cell culture media were characterized. To obtain a particular oxygen concentration, nitrogen plus oxygen gas mixtures generated from a gas manifold (Alicat Scientific, Tucson, AZ), which could be precisely computer-controlled, were purged into cell culture media. The calibration data was used to calculate the oxygen concentration and pH which could be translated from the fluorescence intensities of the optical sensors under an inverted microscope.

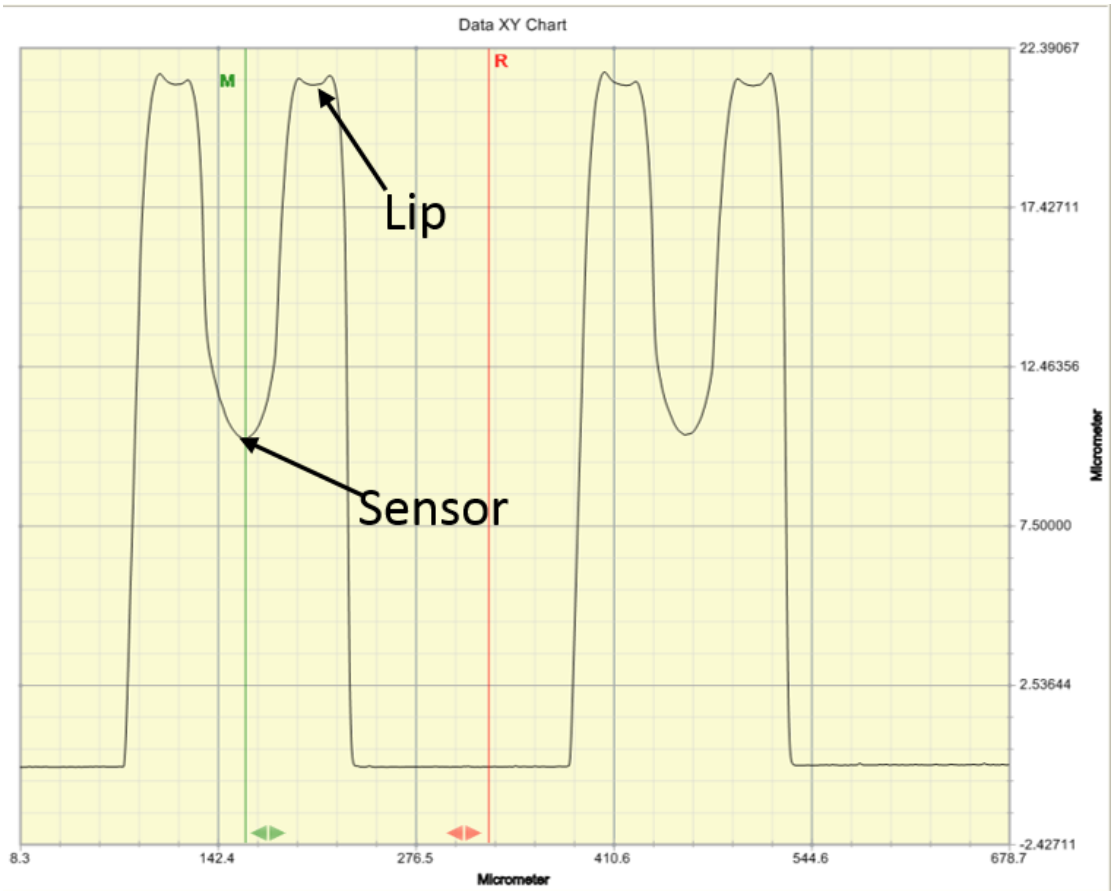

Figure 16. Dektak Contact Scanning on Thermally Polymerized Sensors in Two Microwells (Height of Lips and Sensors).

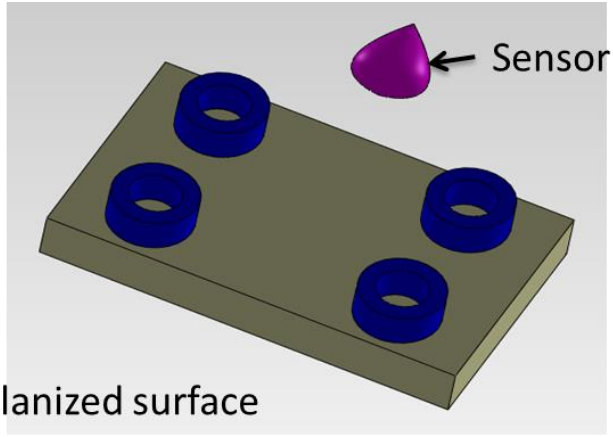

(a)

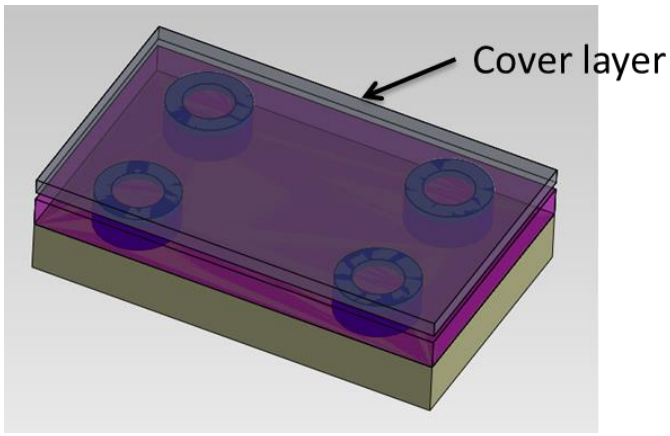

(b)

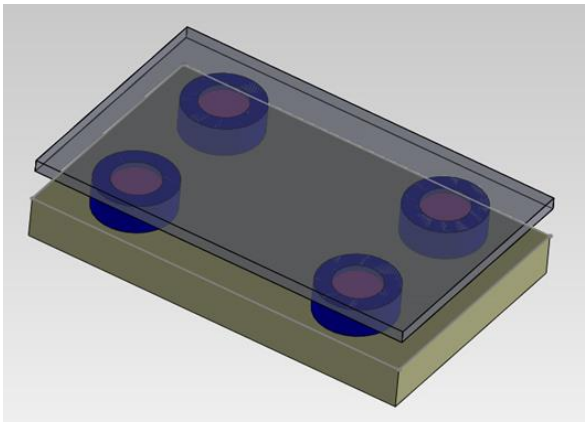

(c)

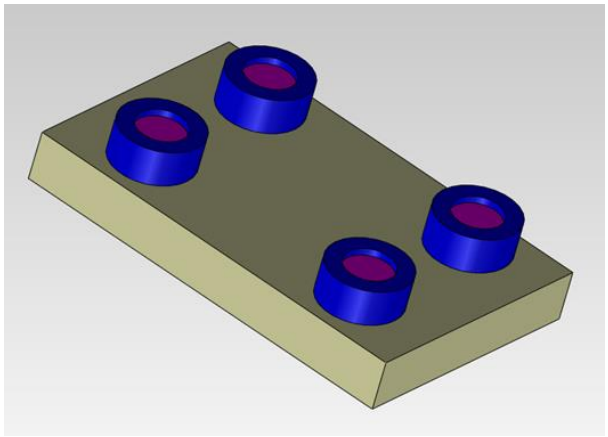

(d)

Figure 17. Sensor Deposition Procedure: (a) Surface Preparation and Sensor Synthesis; (b) Casting a Thin Film of Sensor Liquid Solution on the Modified Surface; (c) Sensor Removal; (d) Sensor Polymerization by UV Curing.

3.2.7 Experimental Setup

The "draw-down" experiment was performed by aligning sensor arrays to the microwell arrays on an inverted fluorescence microscope as described in Section 3.2.3. The overview of the device is shown in **Figure 18**. The central components were the two featured glass chips located at the middle of the main fluid channel, where the 10 × 10 microwells with optical sensors and the cell traps with immobilized single cells were aligned. The fluid flow pathway started from two inputs, with one connected to oil and the other to the cell culture media, directed to microfluidic channels and microchambers formed by the two chips, and finally reached to the outlet connecting a waste bottle. **Figure 19** illustrates how the multiple layers are built to equip the optical sensors and single cells in a microfluidic device.

One critical technique was to manipulate a rapid alignment for the two fused silica chips using an inverted bright-field microscope. A semi-automated assembling apparatus was developed to promote the assembly efficiency and accuracy. The apparatus was basically composed of two modules: an immobile bottom holding the fused silica chip with single cells, and a manual XYZ stage mounted with the fused silica chip with optical sensors. When performing the alignment using the inverted microscope beneath the apparatus, the cell chip was firstly locked at the stationary bottom, and then orientation of the sensor chip was steadily modified along all three axes according to the four pairs of marks at the chip corners (X and Y directions were adjusted prior to Z). When the alignment was completed, the two chips were pressed and the draw-down device was closed by tightening the screws, followed by connecting the plastic tubing to inlets and outlet.

The operation sequence to introduce oil and cell culture media for draw-down experiment is listed as shown in **Figure 20**:

- At the beginning, the inlet connecting to oil was turned off. Fresh cell culture media was injected into the device to provide nutrients and oxygen to the single cells located inside the formed microchambers through the 1 μm gap.
- After 5 minutes, the inlet connecting to cell culture media was switched off. Heavy mineral oil (red color stained) entered the device and gradually displaced the media flowing around the microchambers.
- All the ports of the draw-down device were closed and the device was then placed on the stage of an inverted fluorescence microscope. Fluorescence intensities reflected from the tri-color sensors were extracted for 120 minutes at 1 minute intervals.
- Carbonyl cyanide 3-chlorophenylhydrazone (CCCP) mixed in cell culture medium was added from one inlet into the device, and displaced the preexisting oil in the microfluidic channels. CCCP would enter the microchambers and affect to increase cellular oxygen consumption rate. Then another oil sealing and fluorescence imaging was executed as an enabling approach to implement drug screening.

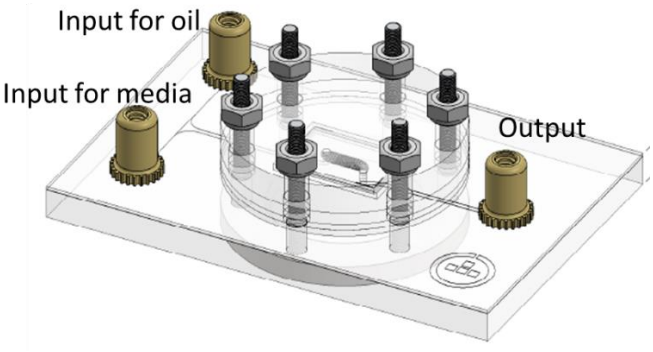

Figure 18. Assembled PMMA Device with Multi-layers Containing Two Featured Chips.

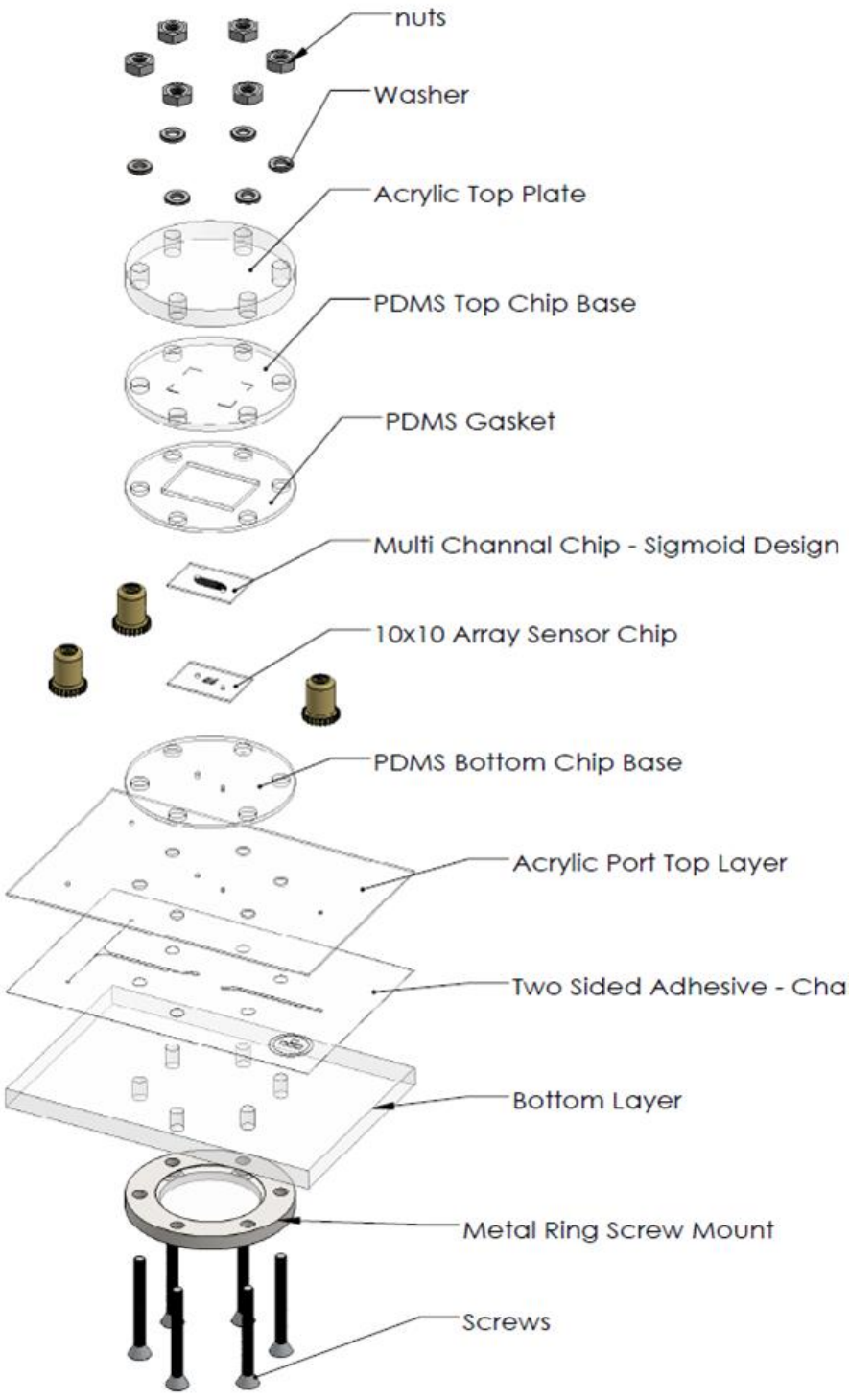

Figure 19. Detailed Demonstration of Draw-down Assembly.

Note: **Figures 18 and 19** are a courtesy of Wacey Teller.

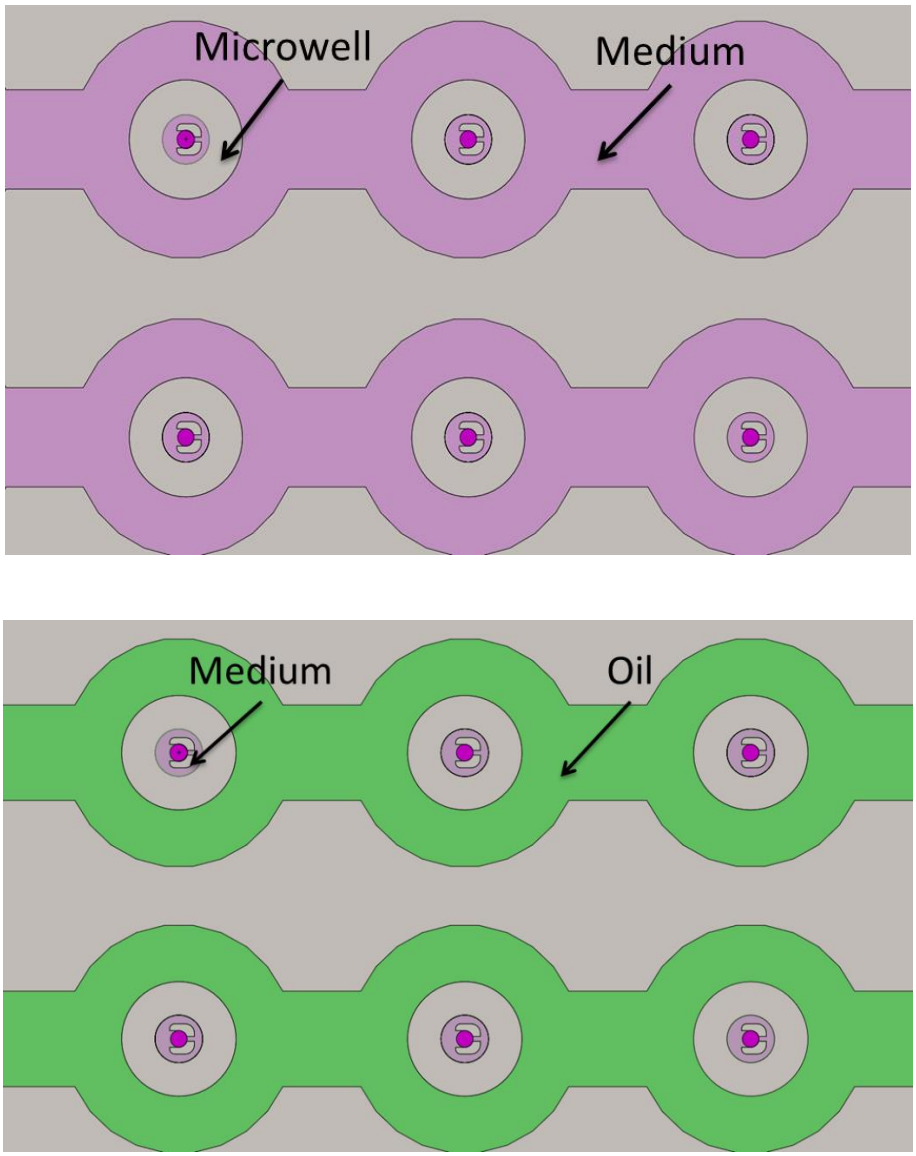

Figure 20. A Diagrammatic Illustration of Oil and Media Flow Process in Microfluidic Channels.

3.2.8 Data Analysis

Fluorescence intensities were measured by data analysis software written using LabView 2014 (National Instruments, Austin, TX).

3.2.9 Summary

In this work, the platform to perform a multi-parameter analysis on single-cell metabolism can be summarized and demonstrated in **Figure 21**. Two fused silica chips with SU-8 micro-fabricated structures, respectively functionalized for trapping single cells and patterning optical sensors, were assembled to form hermetically sealed microchambers using heavy mineral oil. The platform can manipulate simple intensity-based ratiometric measurements and a rapid single-cell loading on a high-throughput matrix, monitor important factors of cellular activities, and provide a promising approach for drug screening.

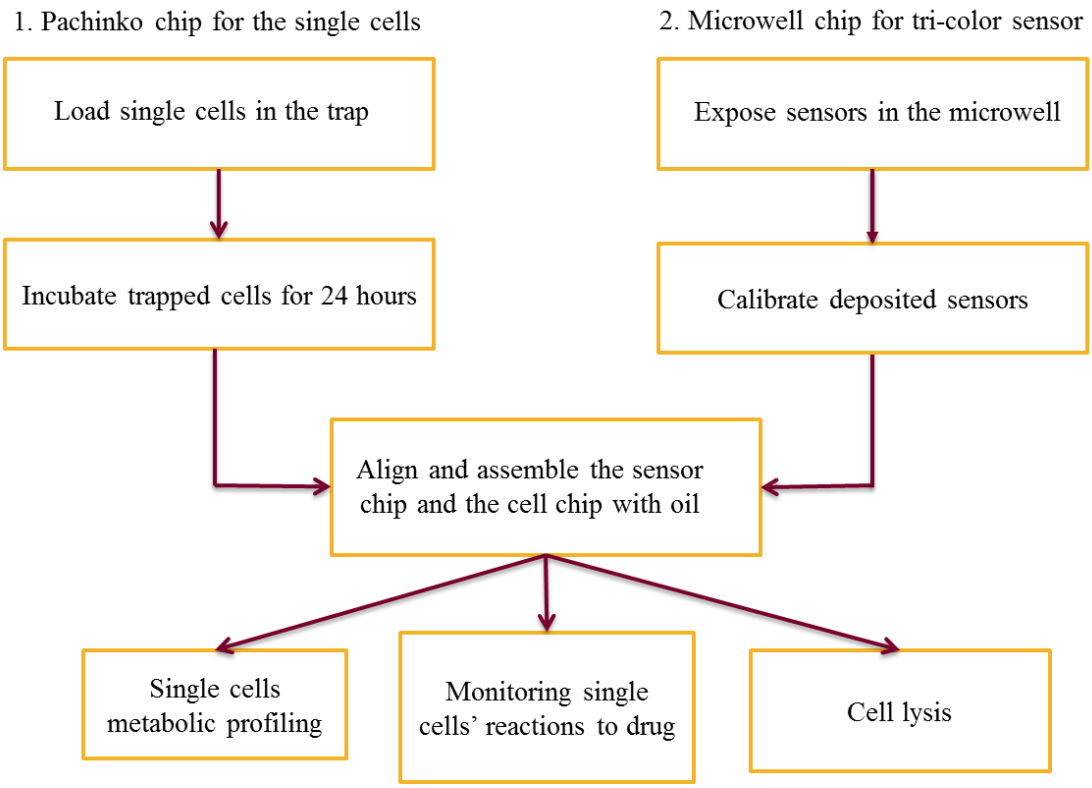

Figure 21. Summary of Platform Design and Work Principle.

3.3 Results and Discussion

3.3.1 Optical Sensor Deposition and Characterization

As described in Section 3.2.6, a synthesized sensor solution was UV irradiated and polymerized in 10 × 10 microwells, and the fluorescence image of the deposited sensors was shown in **Figure 22**. Most of the microwells had isolated sensor dots, but the area outside some microwells had polymerized sensor as well which was caused by an incomplete sensor removal before UV exposure. Because these extra sensors would not reflect any fluorescence alterations during draw-down experiments, this sensor chip could be used for sensor characterization and single-cell metabolic profiling. One key step was to determine the thickness of the sensor after UV exposure. According to the previous knowledge, a longer exposure would generate a thicker photo-polymerizable sensor layer. In the design, the preferred sensor thickness in the microwells was expected to be smaller than 2 μm because thick sensors would increase the gap between the two chips and multiply the possibility of oil entering the microchambers. Three sensor chips were set up and the exposure matrix from 10 seconds to 30 seconds with 10 second intervals was performed, and a five-point measurement was contact-scanned on the sensor chip (**Table 2**). Exposure time of 16 seconds was finally selected and optical sensor dots of averaged 1 μm thickness was deposited.

Table 2. Relationship between Averaged Sensor Deposition Thickness and UV Exposure Time

Exposure Time (s)	10	20	30
Sensor Thickness (μm)	Less than 1	1.5	3.4

The sensitivity of the triple sensor plays a significant role for single-cell metabolic analysis, particularly when monitoring the single cells by evaluating the fluorescence intensity change of the sensors. To characterize sensors sensitivity, a fused silica substrate (16 mm × 11 mm) was patterned with 10 × 10 deposited tri-color sensors and then immersed in a Britton-Robinson (B-R) buffer for the luminescence measurement by an excitation laser. The buffer (pH=7) was purged with gas mixtures containing different oxygen and nitrogen concentrations to set a series of dissolved oxygen concentrations during oxygen sensor characterization. For pH sensor characterization, pH value of the buffer (8.6 ppm oxygen concentration) was varied from 6 to 8. The pH sensor follows a sigmoid function:

$$\frac{I}{I_0} = \frac{m_2 - m_1}{1 + \exp(pK_a - pH)/p} + m_1$$

Where I represents the fluorescence intensity measured at different pH values during the experiment and I_0 represents that at the lowest pH value. m_1, m_2, pK_a, and p are, respectively, the initial value, final value, point of inflection and width of the sigmoid curve. The pK_a value was calculated to be 7.1, which is very suitable for single-cell metabolic experiments. For the oxygen sensor, it follows the Stern–Volmer equation:

$$\frac{I_0}{I} = 1 + K_{svq}[O_2]$$

Where K_{svq} is the Stern–Volmer quenching constant and $[O_2]$ is the corresponding dissolved oxygen concentration. I_0 is the steady state fluorescence signals measured at 0% and I represents various dissolved oxygen concentrations. In this work, as shown in **Figure 23**, when calibrating pH sensor, the sensors array was immersed in five different pH value (6.0, 6.5, 7.0, 7.5 and 8) buffers and the fluorescence intensity was measured and recorded. Then the ratio of the intensities of pH and reference sensors was plotted in terms of pH value as shown in **Figure 23** (a). By the sigmoid function fitting, each spot corresponded to a particular curve with a function. Similarly, the ratio of the fluorescence intensities of reference and oxygen sensors was linearly fitted on the dissolved oxygen concentration (0%, 5%, 10%, 15%, and 20% oxygen) as shown in **Figure 23** (b).

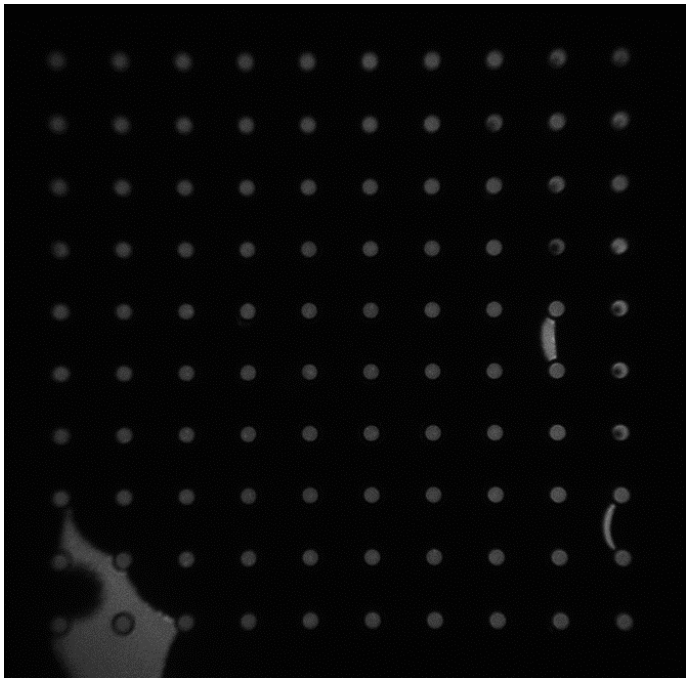

Figure 22. Deposited Sensor Array for Oxygen and pH Calibration.

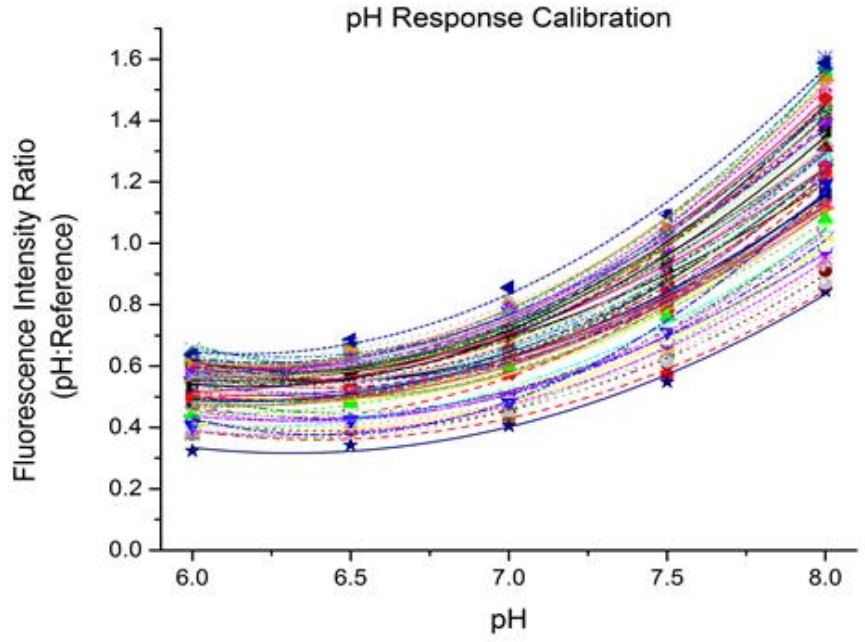

(a)

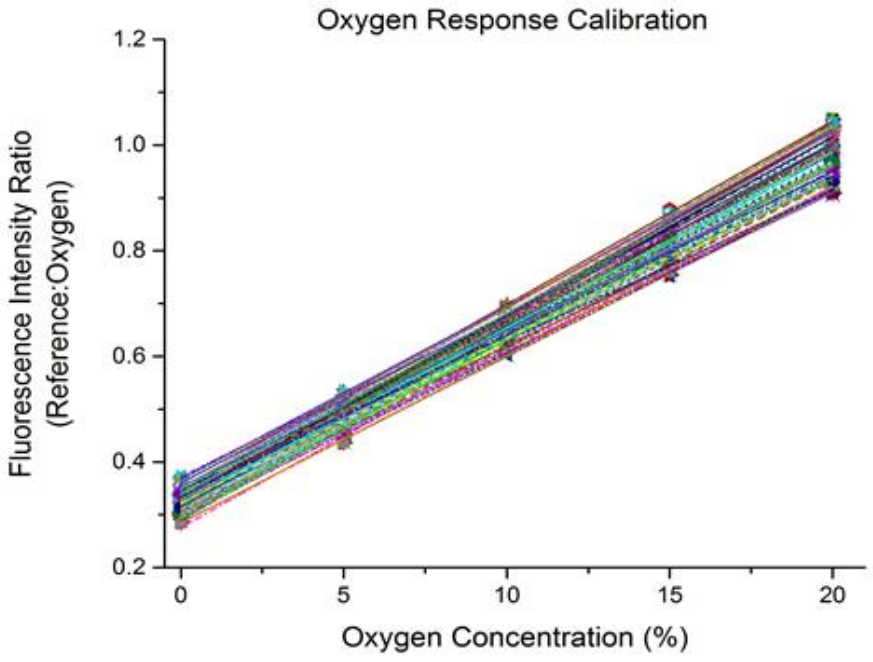

(b)

Figure 23. Calibration of a 10 × 10 Sensor Array: (a) Sigmoid Boltzmann Fitting for pH Sensor Dots; (b) Stern-Volmer Fitting for Oxygen Sensor Dots.

3.3.2 Cell Loading

To achieve a rapid, highly accurate cell immobilization, the microfluidic method was used instead of the piezo-driven pico-liter pump, which was well developed in CBDA and transported single cells into location of interest by aspiration and expiration on a microtip. The main reason was that it already required considerable time to accomplish 3 × 3 microwells using the pico-liter pump, and thus it needed a much faster process to immobilize single cells in 10 × 10 matrix or larger. Microfluidic channel could facilitate rapid isolation of single cells from of a mixture of cells in bulk solution, which was based on laminar flow characteristics driven by valves and pumps. Isolating single cells from bulk solution was carried out by micro-fabricating a "Pachinko"-shaped trap located at the center of a circular area (**Figure 24**), which was designed to establish more relative uniform velocity around the trap than straight channels. A small distance between the lobes was required to allow the stabilized stream pass through and trap the larger individual cells (in terms of the distance).

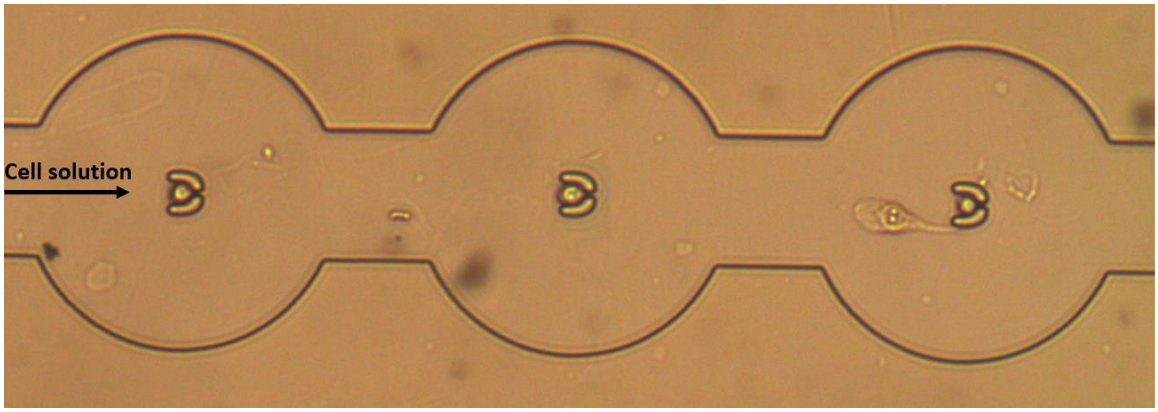

Figure 24. Bright-field Micrograph of Single-cell Immobilization by Cell Traps in Microfluidic Channels.

The entire cell loading time for this design was about 1 minute on average. When a desired occupancy (90% plus) of trapped single cells was observed under bright-field microscope, hydro-dynamical flow through the microchannels was stopped. . After a 24-hour incubation to allow the cells for attaching on the traps and recovering from potential stress caused by operation, the viability of the cells was assessed by imaged the cells stained using the LIVE/DEAD® Cell Imaging Kit (488/570) under a confocal microscope. As seen in **Figure 25**, two dead cells appeared (during incubation or even cell loading) on the traps, and 91% of the live cells adhered on the SU-8 traps which would be completely covered by the microwells after chip alignment.

(a) 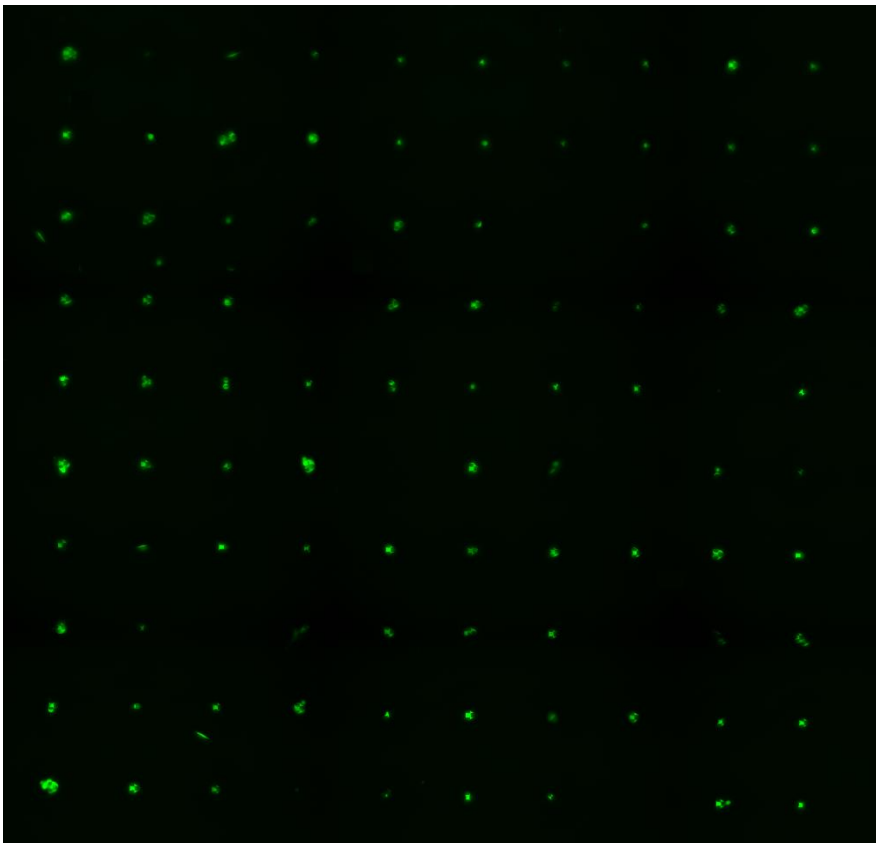

(b) 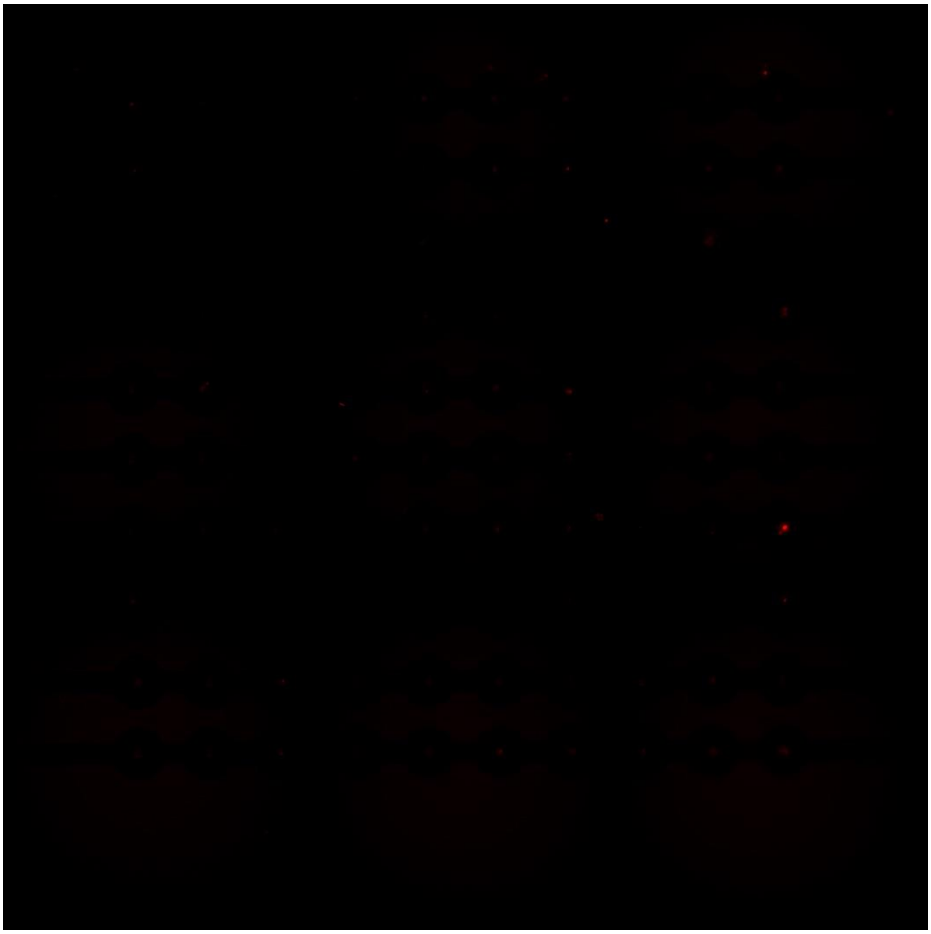

Figure 25. Assessment of Cell Viability by LIVE/DEAD® Cell Imaging Kit (488/570) after 24 Hour Incubation: (a) Green Stained Live Cells; (b) Red Stained Dead Cells.

3.3.3 Fluid Pathways in Device Channels

When the cell chip and sensor chip were prepared, the two chips were assembled as described in Section 3.2.7. The vital process to execute single-cell analysis profiling in the design was using mineral oil to seal the microchambers. However, whether oil would enter the microchambers and then affect normal cellular response measurements became a consequential concern. According to the simulation (exactly same dimension) by COMSOL Multiphysics® (COMSOL, Burlinton, MA) in **Figure 26**, when flushing mineral oil into the channels, continuous flow velocity outside the microwell was

observed and there was no velocity inside the microwell (dark blue reflects a velocity of nearly zero while light blue, yellow or red reflects velocities above zero), indicating that the mineral oil only flowed around the microwell.

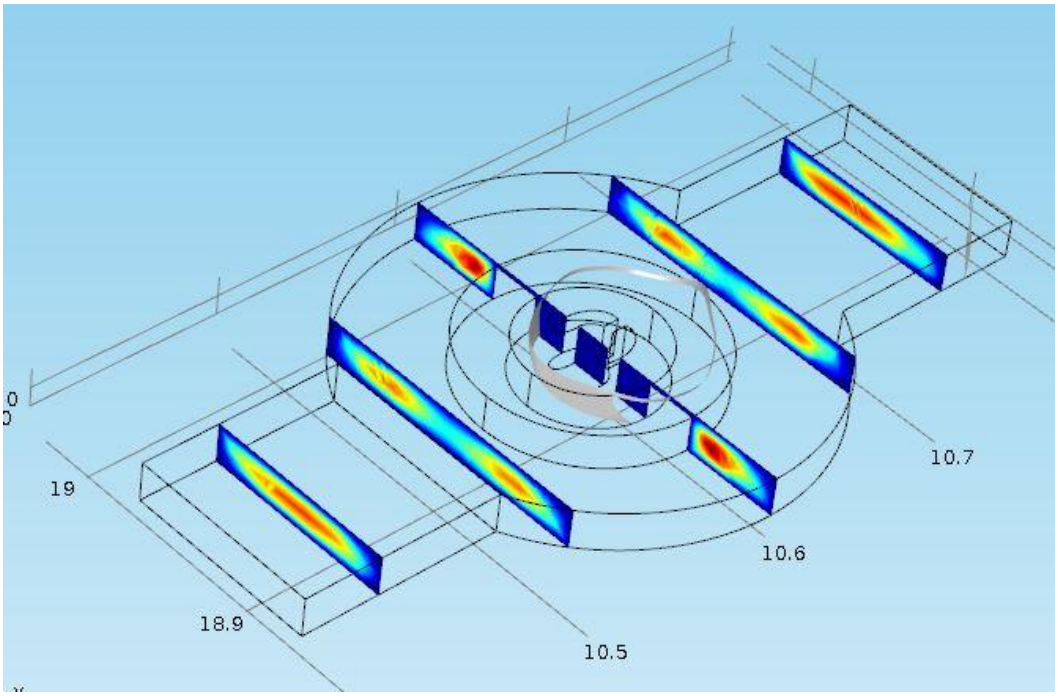

Figure 26. Fluid Velocity Simulation on the Microchannels (Dark Blue: Zero Velocity; Light Blue/Yellow/Red: 0.2 – 1 m/s). (Courtesy of Manoj Sreenivasulu.)

(a) 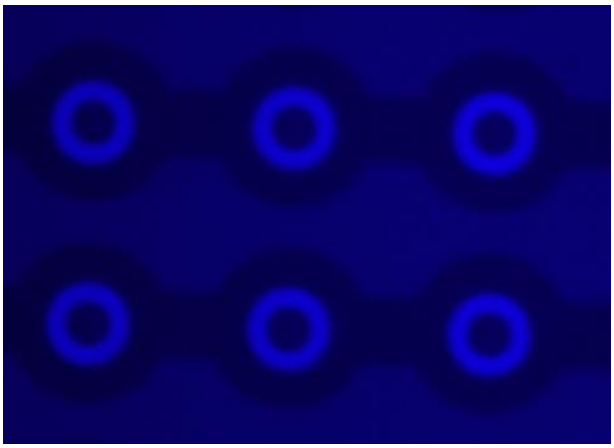

(b)

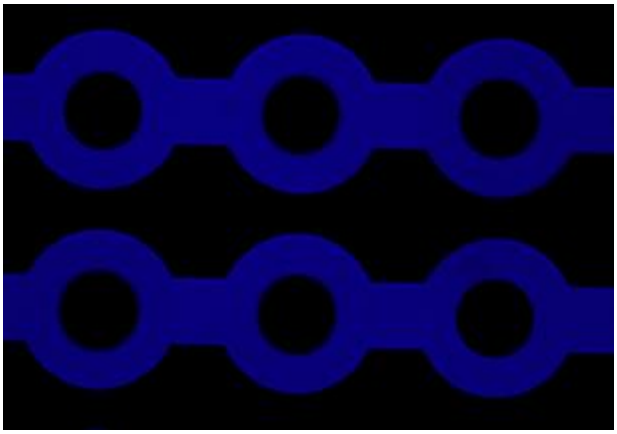

(c)

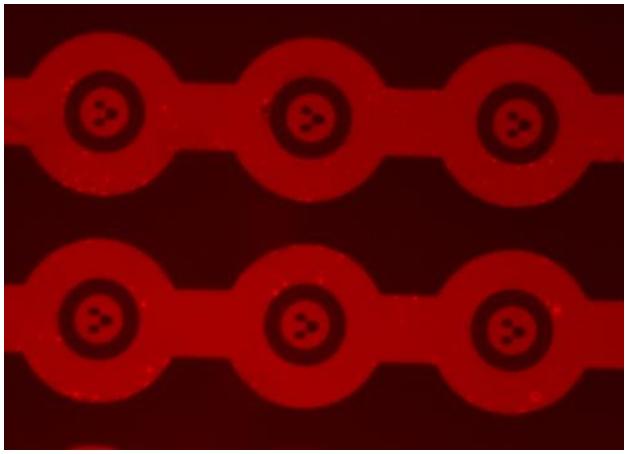

(d)

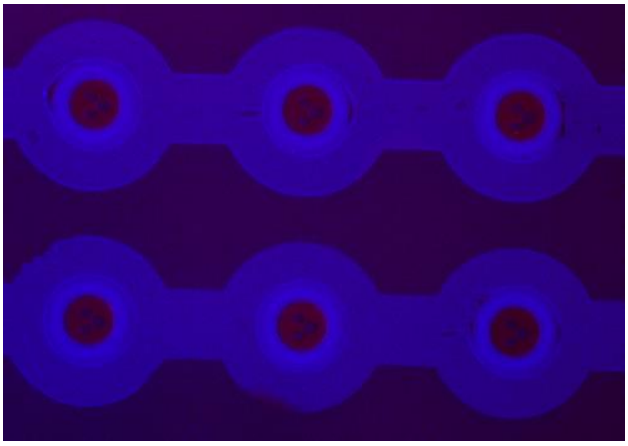

Figure 27. Oil and Cell Culture Media Flowing Situation: (a) Regular Media into Channels and Microwells; (b) Blue-Stained Oil Flowing around Microwell; (c) Red-Stained Media Displacing Oil and Entering Microwell; (d) Second Time of Stained Mineral Oil Addition.

As demonstrated in **Figure 27**, to figure out how fluids flowed in the assembled draw-down device, regular cell culture media was firstly introduced into the channels from the inlet and entered the microchambers. Under the fluorescence microscope, there was only a weak intensity from SU-8 pattern auto-fluorescence. Then heavy mineral oil was stained by a fluorescent polymer (synthesized by Dr. Zhang) (Zhang, Su et al. 2016) and flowed around the microchamber without entering chamber. This result demonstrated that heavy mineral oil could be used as a sealing material with the goal of enclosing the formed microchambers containing single cells and optical sensors. Another critical principle needed to be proved was whether cell culture media could displace the mineral oil and enter the microchambers, because it would allow to study drug effects on the same cells. Rhodamine was used to dye the cell culture media and the results were shown in **Figure 27** (c) and (d). In summary, the second cell culture media (also could be mixed with drug) was fully blended into the microwells and hermetically sealed by mineral oil once again. According to this property, when the single cells were immobilized in the microchambers, by repeating the above steps various drugs could be applied to the same cells, and the reaction of the same cells to each drug would be monitored under the fluorescence microscope imaging.

3.3.4 Single-cell Metabolic Profiling

The draw-down experiment was performed to measure the characteristic oxygen consumption and pH variations in real-time. Significant cell-to-cell differences were observed in the alterations of the fluorescence intensities from optical sensor arrays in **Figure 28**. The measurements were automatically collected for 120 minutes at 1 minute

intervals on an inverted microscope. From the obtained intensities, the data were calculated and transferred to the change of pH value and oxygen concentration inside the sealed microchamber by calibrating the relationship between reference-probe and oxygen- or pH-probes as shown in **Figure 28** (c) and (d). From the curves, the time needed to consume all of the oxygen in each microwell differed from each other, including some cells that exhibited no respiration kinetics. The pH value in the microchambers kept decreasing during 120 minutes, and the slopes of the curves presented different hydrogen ion production rate of individual cells. These variabilities in OCR and ECAR were caused by intrinsic intercellular heterogeneity. The observed OCR and ECAR variations and the differences in single-cell OCRs and ECARs displayed the importance to study cell-to-cell heterogeneity and confirmed the need for single-cell studies. Based on the platform mechanism, the single-cell metabolic analysis could be developed from 10 × 10 matrix to 20 × 50 or larger designs on a larger fused silica chips.

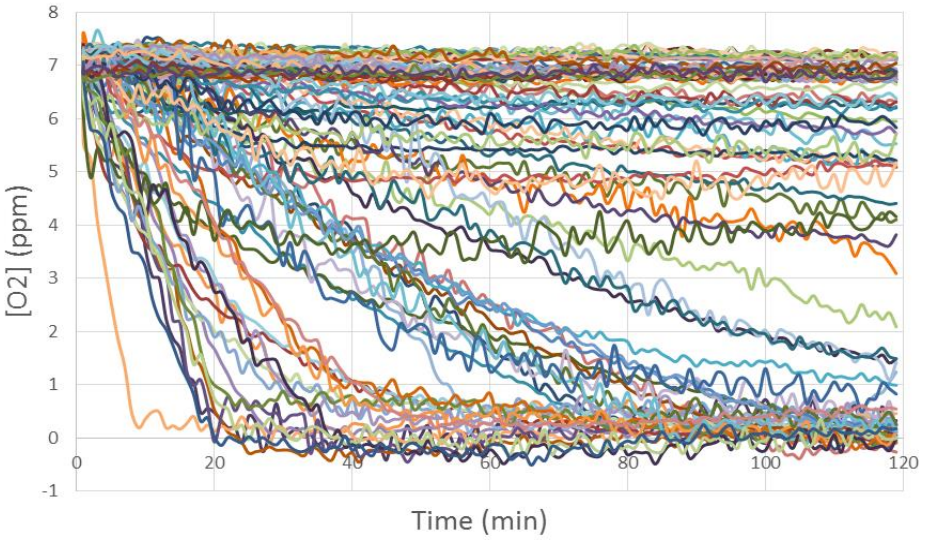

(a)

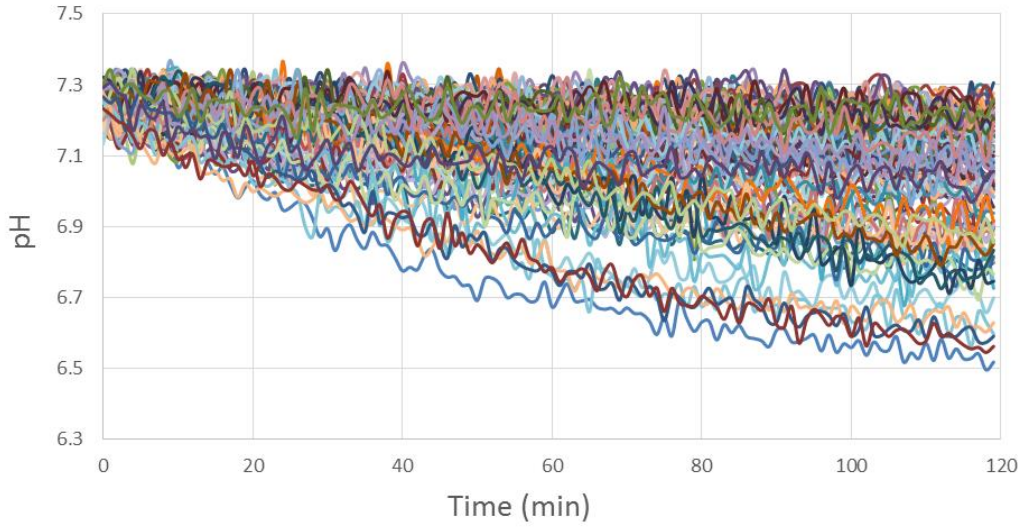

(b)

Figure 28. Single-cell Metabolic Profiling: (a) Oxygen Consumption and (b) Acidification Kinetics.

3.3.5 Drug Response of Individual Cells

Studying drug cytotoxicity plays a significant role in dissecting disease status in individual cells and developing innovative treatment strategies.(Enriquez-Navas, Wojtkowiak et al. 2015) The platform designed could be used for drug screening assays to identify the aberrant response of the single cells, and explore underlying molecular mechanisms. Most importantly, the device allows drug screening on the same cells by means of the repeatable media exchange across the channels and microchambers. In this work, carbonyl cyanide 3-chlorophenylhydrazone (CCCP), an uncoupler of the oxidative phosphorylation was used as the drug stimulation to compare the respiratory rate of trapped single cells in the sealed space with and without drug through extracting fluorescence intensities from the optical

sensors, since CCCP treatment can disrupt mitochondrial potential and increase cellular oxygen consumption even in the hypoxia-treated cells. If the single cells' reactions to the stimulus of CCCP can be successfully performed and monitored on the device, this platform has the potentials to study individual cellular responses to other drugs which can significantly benefit to disease treatment especially cancer therapy.

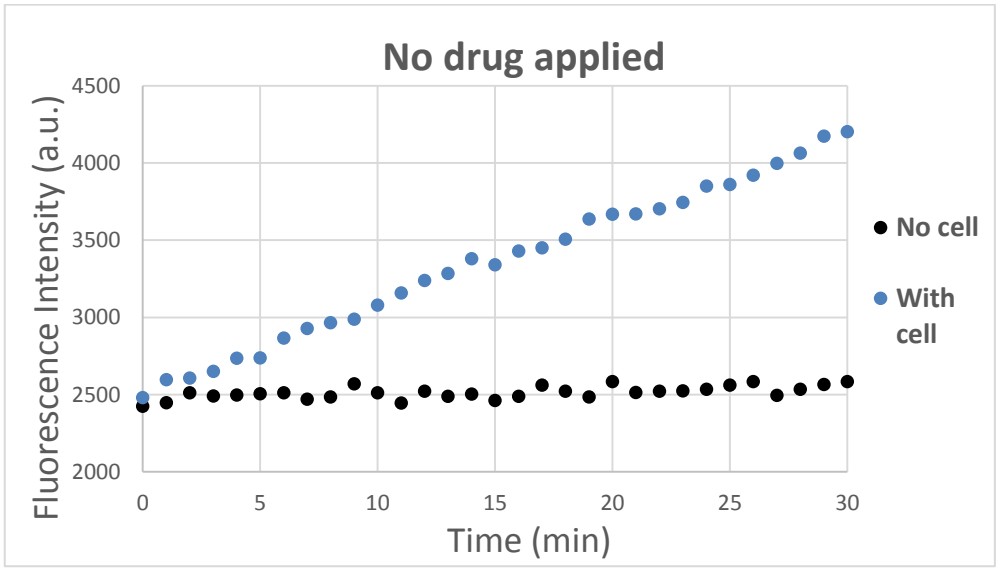

(a)

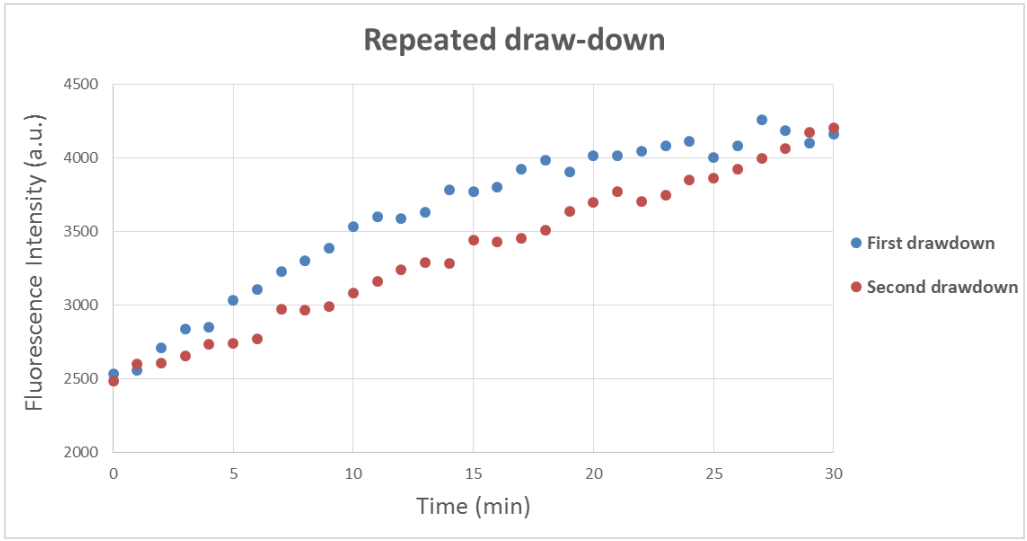

(b)

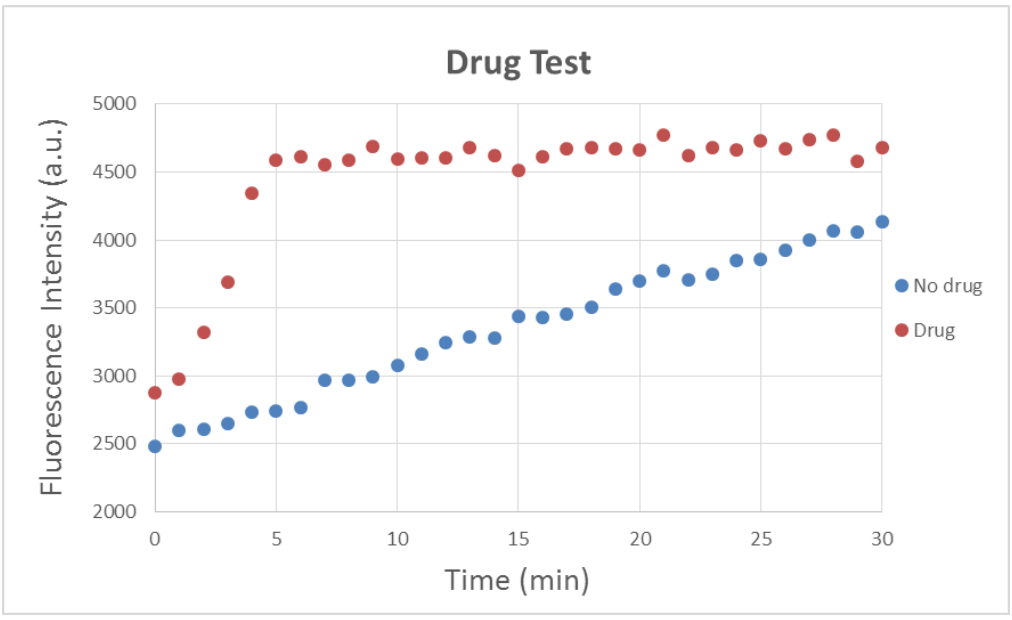

(c)

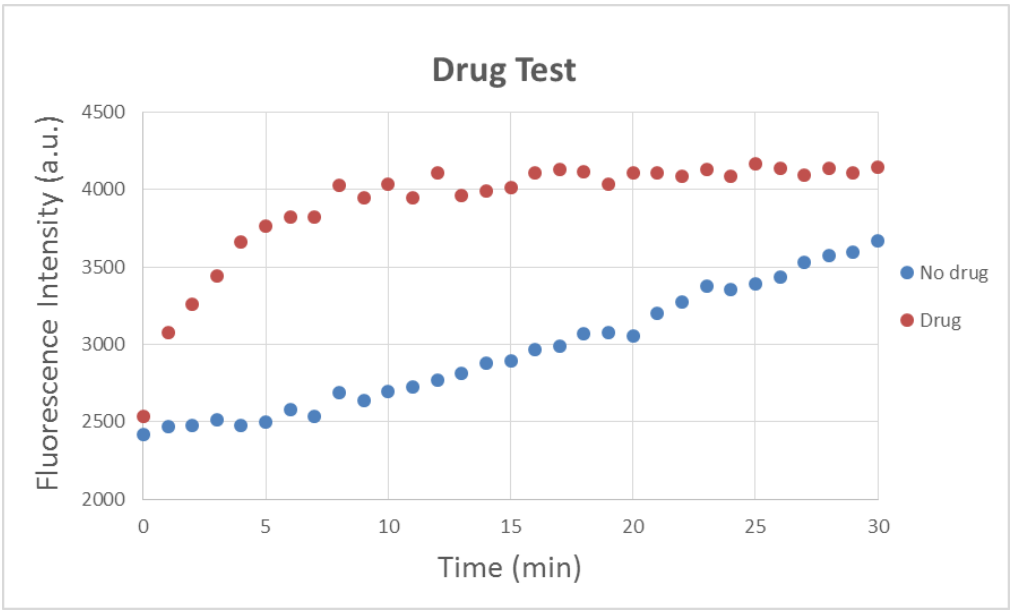

(d)

Figure 29. Drug response: (a) Fluorescence Intensity Monitoring on a Microwell with a Single Cell and a Microwell without Cells (no CCCP); (b) Repeated Drawdown without Adding CCCP; Drug Application on Two Different Cells (c) and (d).

The procedure to prepare CCCP in cell culture medium was: 1) weighing 204.6mg CCCP powder in 1 mL Dimethyl sulfoxide (DMSO) to compound a 1 mM concentration; 2) Add 30 uL of 1 mM CCCP per 1 mL culture volume to the untreated A549 cell solution of total 3 mL. The chip loaded with the single A549 cells was assembled and aligned to the 10 × 10 array of tri-color sensor inside the microwells in draw-down device, hermetically sealed by the heavy mineral oil. Once the mineral oil flowed around the microwells, the device was moved to an inverted microscope for 30 minute fluorescence data collection. Afterwards, the mineral oil in the channels was displaced by fresh cell culture media and incubated for 1 hour to supply nutrients and oxygen to the single cells through the gap formed between the two chips. Then the diluted CCCP was added into the channels and blended into the microwells. By manipulating another 30 minute draw-down fluorescence profiling, the same cells' response to CCCP was analyzed and compared to the previous measurements. Two negative control experiments were performed before adding CCCP into the microfluidic channels: (a) comparison of oxygen responses between two microwells, one contained one single cell and one had no cells; (b) repeated draw-down steps (using mineral oil to seal the single cell twice and each for 30 minutes) manipulated on the same cell. These two experiments were used to illustrate oxygen consumption of the single cell and optical sensor responses when two different fluid (media and oil) alternately flew inside the device without CCCP (**Figure 29** (a) and (b)). Particularly the repeated draw-down did not have an obvious influence on the single cell's oxygen consumption speed in the same sealed microwell. Therefore, if CCCP was added into the channel and stimulated the single cells, and significant changes of OCR were observed (**Figure 29** (c) and (d)), it proved that the metabolic activities of the single cells were affected by the

external molecules and drug screening could be potentially executed on the device. According to the curves in **Figure 29**, the oxygen consumption rate of the single cells increased after the drug CCCP applied on the cells.

3.4 Summary

In this chapter, the measured and calculated data demonstrated the capability of the experimental approach to perform robust metabolic phenotype characterization at the single-cell level such as OCR and ECAR. More metabolic parameters could be monitored if other optical sensors can be embedded into the device. In addition, the platform exhibited immense potentials to manipulate varieties of drug screening experiments on the same cells with converting fluids (media and mineral oil) into the assembled device.

4. MICROFABRICATION OF LOW-COST THERMOPLASTIC MICROFLUIDIC DEVICE FOR SINGLE-CELL METABOLIC PROFILING

4.1 Background

Modern drug discovery and cellular heterogeneity analysis require fast data collection of multi-parameter measurements on large numbers of samples. (Manz, Harrison et al. 1992) As discussed in Chapter 3, microfluidic devices provide the approaches to high-throughput single-cell metabolic analysis and drug screening. According to the configuration design, the sealing based on mineral oil allows small sample volume in multiplexed microchamber containing immobilized single cells and optical sensors. Glass substrates are widely applied in microfluidic systems since fabrication methods had been well developed by the semiconductor industry, but cost of building platform in glass is not commercial friendly because in the biological application single-use chips are highly preferred to eliminate the need for reuse and cleaning. Therefore, compatibility and applicability of microfluidic devices in these studies lead to developing low-cost techniques in fabrication procedure for mass production. (Rossier, Schwarz et al. 2000) To fabricate disposable low-cost chips, polymer-based microfluidic devices are very attractive by introducing plastics to reduce dependence on a clean room and simplify manufacturing procedures.

Cyclic olefin copolymer (COC) and polyethylene terephthalate (PET) are frequently used in microfluidic systems, which present features with chemically robust, low-cost, biocompatibility and good transparency for optical imaging. Surface modification of plastic substrate is usually necessary for stabilizing and settling live cells by either

physically plasma treatment or chemically coating. Gas permeability is another considerable factor in the multiplexed structures since no gas leakage through the substrate is desirable to seal the single cells. (Koivula, Jalkanen et al. 2016) This is main reason why using COC or PET instead of commonly used PMMA to fabricate the cell loading chip and sensor chip. Plastic materials even have better tolerance to unexpected particle during assembly than SU-8 and KMPR patterns.

Plastic molding techniques relying on hot embossing process are developed to imprint on plastics. In this process, a micro-structured mold is pressed into thermos-plastic polymers and the polymers are heated beyond it glass transition temperature. An inverted replica of the micro-structured mold is imprinted on the plastic surface, and demolded from the mold when the operating tool is cooled down. Thus, from one single mold large numbers of plastic replicates can be rapidly produced. As shown in **Table 3**, to fabricate featured micro-structures on a 4-inch wafer with 32 dies, the operating time is 60 and 30 hours, respectively for a glass wafer and a plastic wafer. Many process steps (RCA cleaning, photo-resist coating, photolithography, development, chrome vapor deposition, wet etching) are involved in glass wafer fabrication. Silicon etch, electroplating, hot embossing are the main steps to imprint plastic wafers. In addition, to acquire new wafers, the fabrication needs to be started over for glass chips, while only a step of hot embossing is needed for plastic chips because the fabricated mold can be reused for mass production. In terms of the cost of substrate material, plastic polymers are of the order of 0.2 – 2 cent per cm^2, while glasses are of the order of approximately 10 – 40 cent per cm^2. In conclusion, plastics replication exhibits a significant advantage of fabricating low-cost chips for microfluidic applications, especially when mass production is required.

Table 3. Comparison of Fabrication Time to Produce Patterned Chips between Using Glass and Plastic Materials

Material applied in microfluidics	Fabrication time (hour)
Glass-based device	30
Plastics-based device	0.25

4.2 Platics Replication

4.2.1 Deep Silicon Etch

Due to the harsh operation in hot embossing, a permanently micro-structured metal mold is usually repeatably used to boss polymeric thermoplastic substrate. To imprint micro features on metal surface, a standard nickel sulfate galvanic process to convert the micro structures from silicon template is selected, which has low brittleness and tensile stress sensibility in hot embossing. The detailed procedure of micor-patterning on silicon wafers is described in **Table 4** and **Figure 30**. Basically, the silicon surface was firstly deposited with a thin film (20 μm) of SU-8 3025, followed by photolithography pattering. Then SU-8 functioned as a masking layer, transferring microstructures to silicon by an inductively coupled plasma reactive ion etching system with high-aspect-ratio silicon etching performance. **Figure 31** shows a 20 μm micro structure fabricated by reactive ion etch on a silicon wafer, which can be hot embossed by the nickel tool from electroplating.

Table 4. Deep Silicon Etch Procedure

Important steps	Detailed parameters
Wafer preparation	• RCA cleaning • Dehydrate at 160° C for 30 minutes • Surface treatment by oxygen plasma for 10 minutes at 200 W and 300 mTorr
SU-8 patterning	SU8 3025: • Spin-coat: 4000 rpm for 20 µm thickness • Softbake: 1 minute at 65° C and then an infinity (>5° C/minute) ramp to 95° C and hold for 10 minutes on a hot plate; cool to room temperature (R.T.) • Exposure: 225 mJ/cm^2 with and i-line filter • Post Exposure Bake: Ramp at infinity to 95 °C from R.T. • Develop for 4-5 minutes with agitation and inspection • Hardbake: Ramp at infinity to 150 °C.
Silicon etch	• Etch time: 20 minute • Etched thickness: 20 to 21 µm • SEM imaging

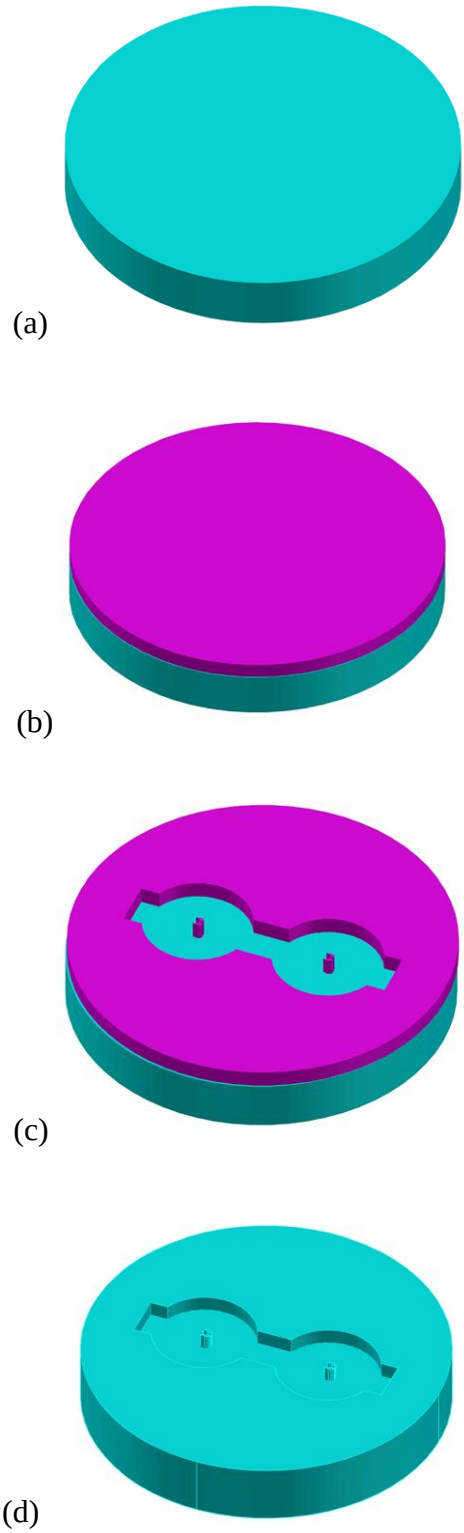

Figure 30. Deep Silicon Etch Procedure: (a) Silicon Surface Cleaning; (b) SU-8 Thin Film Depostion; (c) SU-8 Patterning on Silicon Surface; (d) Deep Silicon Etch.

(a)

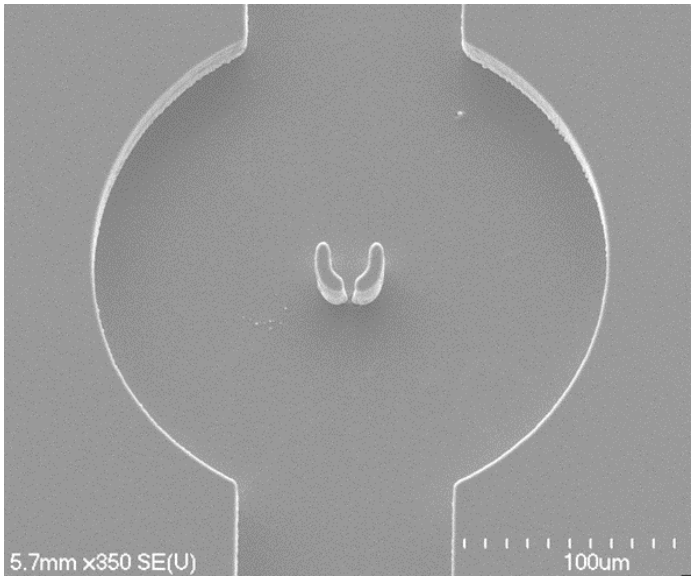

(b)

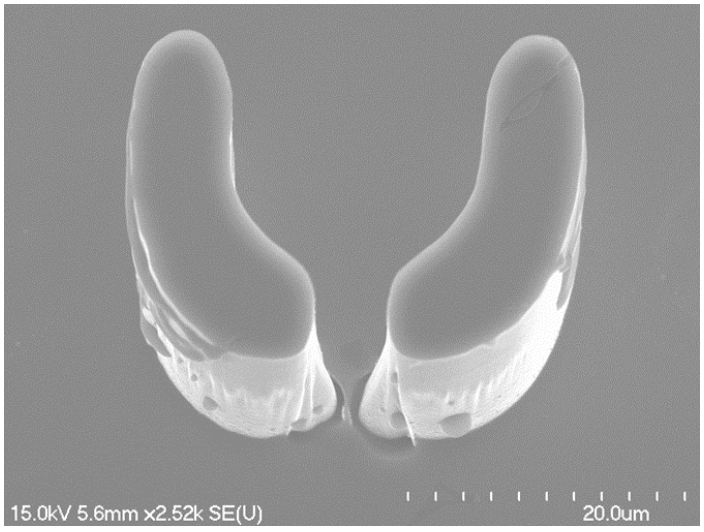

Figure 31. SEM of a Micro Structure Etched into a Silicon Wafer.

4.2.2 Hot Embossing

A thin titanium layer (10 nm) followed by 10 nm gold were sputtered onto the micromachined silicon wafer to provide enough conductivity for electroplating. Then nickel was electroplated generating the mirrored mold which finally was converted to plastic polymers (COC). The procedure is shown in **Figure 32**, and the resulting plastic

micro structures dimensions were the exact patterns of silicon mold. With hot embossing methods, With hot embossing methods, the nickel stamp had a very long lifetime and could be reused for many times to rapidly fabricate thousands of plastic microfluidic devices. The fast replication and release processes provided a low-cost mass production of single-use plastic chips. In **Figure 33**, the micromachined silicon, nickel and plastic wafers were imaged after silicon etch, electroplating and hot embossing. Finally the plastic wafer was diced into 16 × 12 mm dies by TNC, and the dies with microchannels were used for single-cell immobilization and dies with microwells were used to deposit optical sensors.

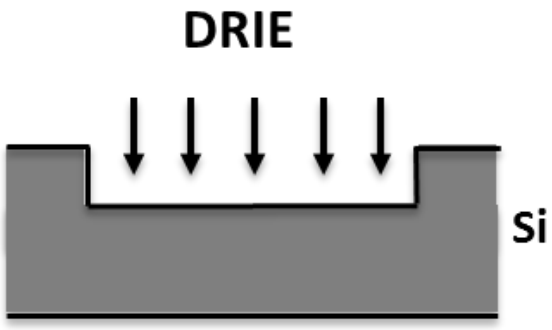

(a)

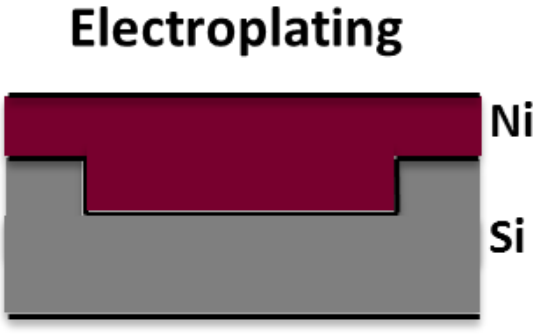

(b)

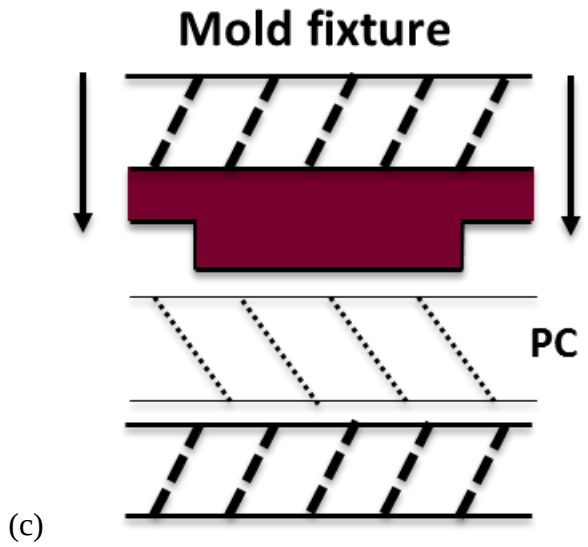

(c)

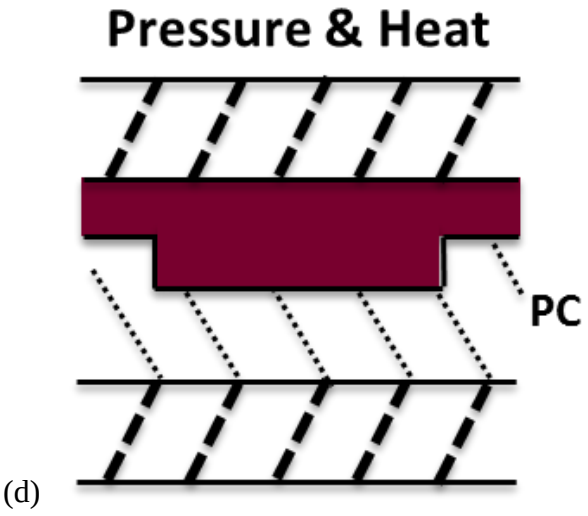

(d)

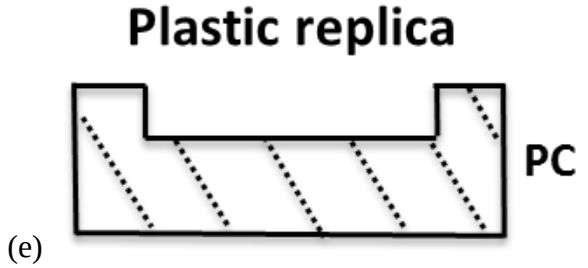

(e)

Figure 32. Plactic Repliation Procedure: (a) Deep Silicon Etch; (b) Electroplating; (c) Hot Embossing Set Up; (d) Embossing above Glass Transition Temperature; (e) Demolding.

(a)

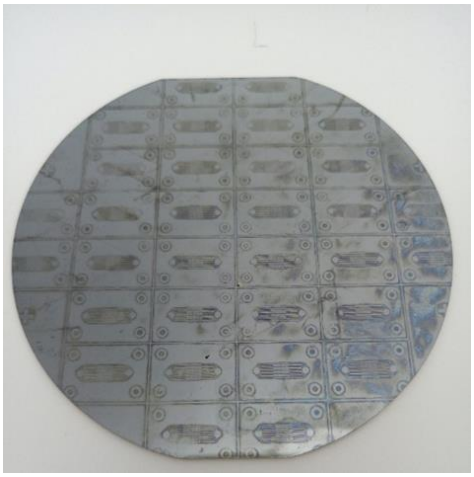

(b)

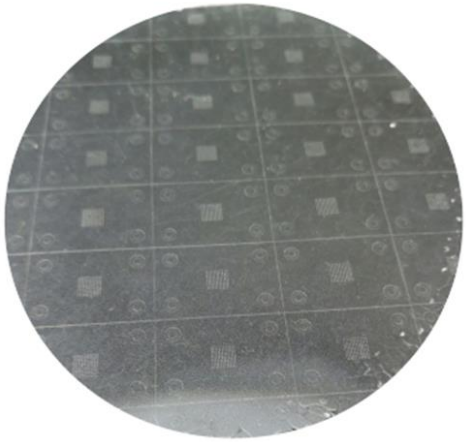

(c)

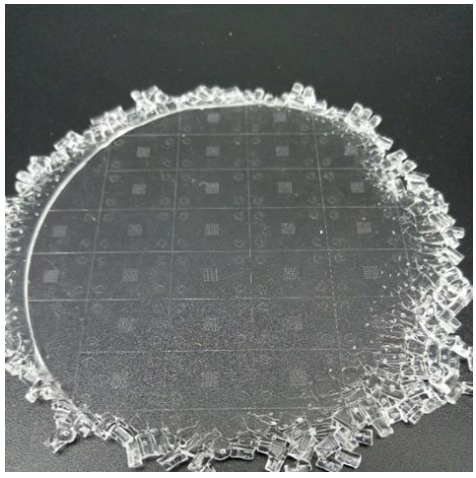

Figure 33. Images of Micromachined Four Inch Wafer: (a) Silicon Wafer after Silicon Etch; (b) Nickel Wafer after Electroplating; (c) Plastic Wafer after Hot Embossing.

4.3 Cell Loading

The cell loading device was very similar to the one used in Chapter 3, with the plastic chip located at the center, connecting one inlet and one outlet. When the single cells in bulk solution were injected from a syringe to the device, they were too small to pass through the traps and immoblized in a 10 × 10 matrix positions. Due to the insufficient surface modification causing a relative low flatness, a modified PDMS layer by Lipidure-CM was added between COC and top PMMA lid (**Figure 34**), since the commercial product is cell-repellant. To have better cell adhesion on the surface, a 10 minute plasma treatment was applied on the COC chip. After an eligible cell occupancy was observed, the plastic chip with trapped cells was moved to incubator for a 24 hour cell growth. Afterwards, LIVE/DEAD® Cell Imaging Kit (488/570) was used to stain the cells for cell viability assessment (in **Figure 35**).

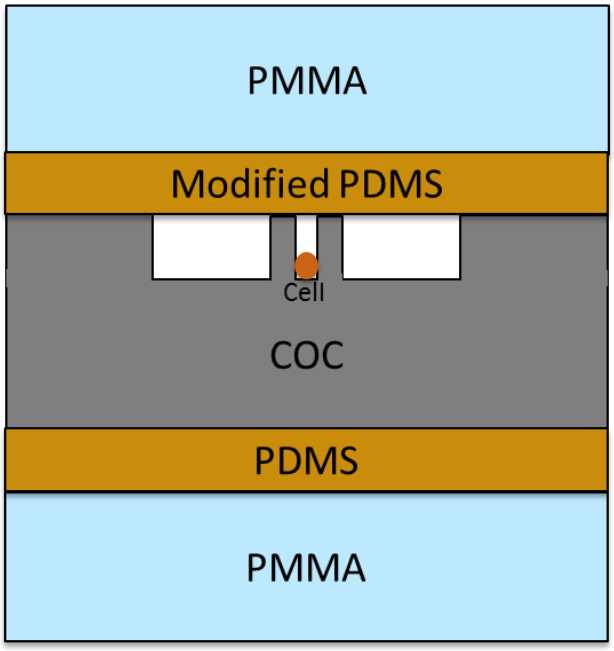

Figure 34. Cell Loading Configuration with Micromachined COC Chip.

(a)

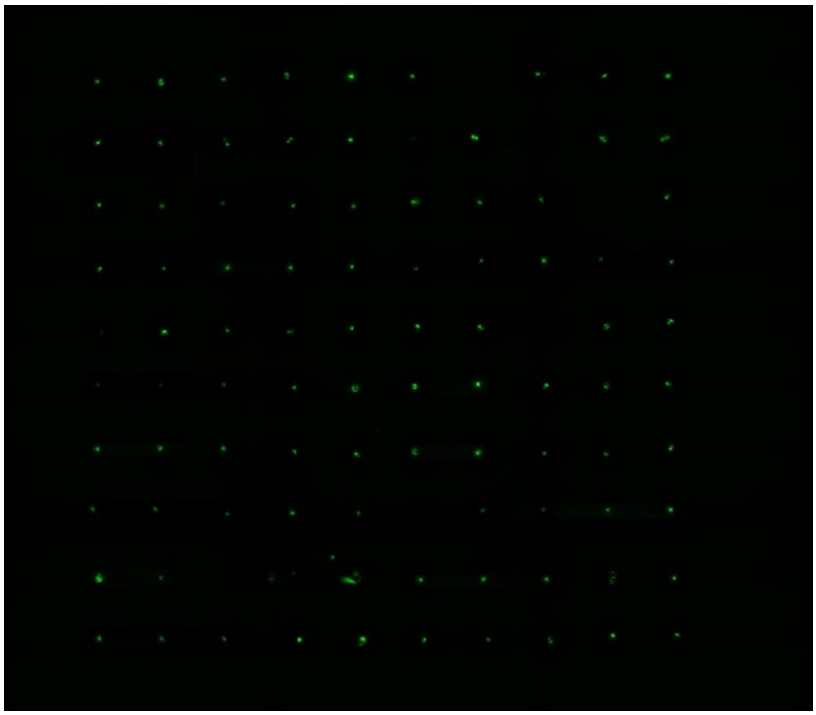

(b)

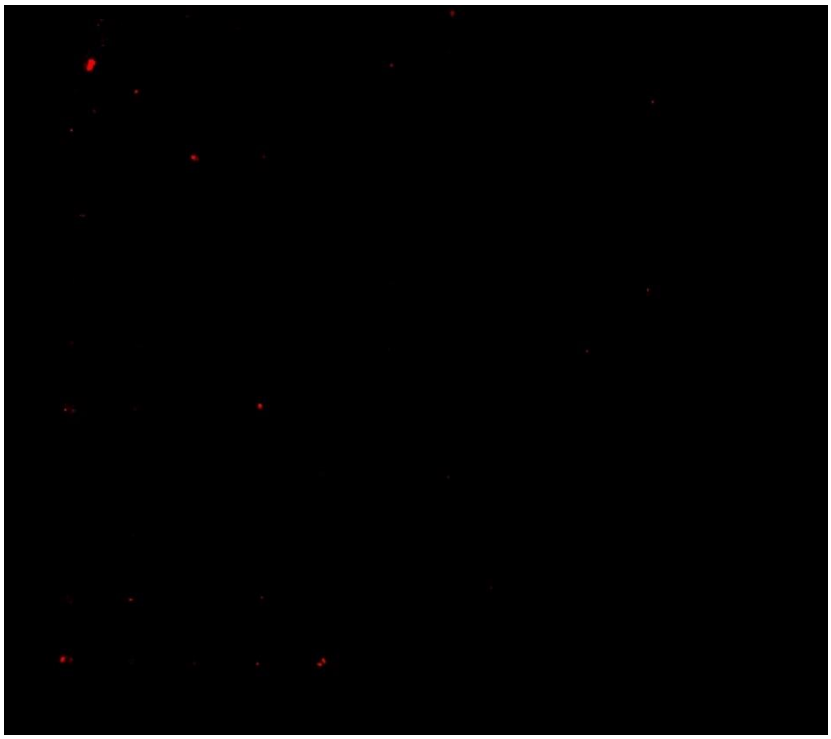

Figure 35. Assessment of Cell Viability by LIVE/DEAD® Cell Imaging Kit (488/570) On Plastics after 24 Hour Incubation: (a) Green Stained Live Cells; (b) Red Stained Dead Cells.

4.4 Single-cell Metabolic Profiling

The draw-down experiment was performed by aligning sensor arrays to the micro-trap arrays hermetically on an inverted microscope. When the optical sensors were deposited in the microwells, the sensor chip was assembled to the incuabted single cells, sealing by heavy mineral oil. The measurements were automatically collected for 120 minutes at 1 minute intervals on an inverted microscope. As seen in **Figure 36**, variations of the fluorescence intensities from optical sensor arrays were observed to indicate cell-to-cell difference for the single cells in the device. From the curves, oxygen consumption rates of the single cells in different microchambers were varied, including some cells exhibited no respiration kinetics. The pH value in the microchambers was reflected by reduction of fluorescence intensities of otpical sensors, and the slopes of the curves presented different hydrogen ion production rate of individual cells..

(a) 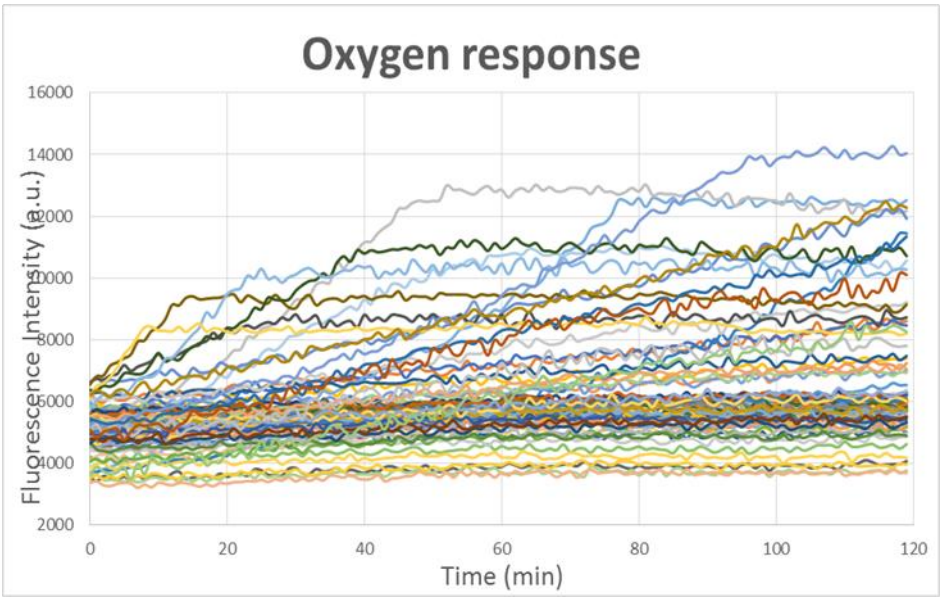

(b)

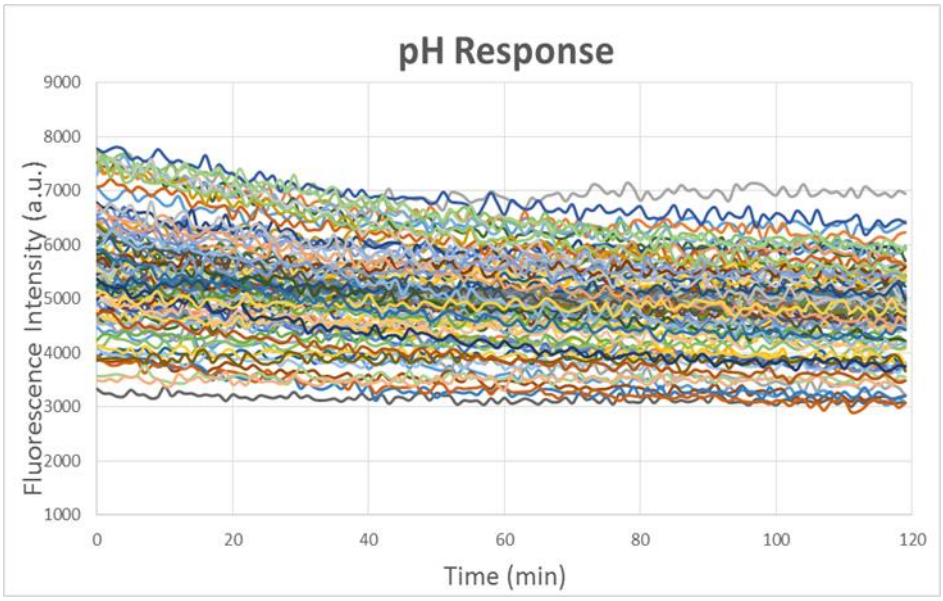

Figure 36. Single-cell Metabolic Profiling on Plastic Chips: (a) Oxygen Response; (b) pH Response.

4.5 Summary

A rapid procedure for the manufacture of optical quality microfluidic devices in COC for single-cell metabolic analysis has been demonstrated. The microsturctures were fabricated using silicon etch, electroplating and hot embossing techniques. Compared to the demonstrated glass fabricaiton in Chapter 3, plastic materials exhibit a significant advantage of a much lower cost process for mass production. The thermoplastic replication process provides a promising approach to benefit to create database based on collecting large numbers of single-cell metabolic parameter measurements,

5. CONCLUSION AND FUTURE WORK

5.1 Conclusion and Contributions

In this thesis, to analysis cellular multi-parameter metabolism at single-cell level, several enabling microfabrication technologies were developed. The basic principle to manipulate the metabolic profiling is to create hermetically sealed microchambers containing single cells and optical sensors. By calculating pH and oxygen responses of the sensors, oxygen consumption and extracellular acidification kinetics of the single cells in the microchamber were measured. To address the challenges in current approaches, improved platforms based on microfluidic techniques were developed.

In Chapter 2, tricolor sensor arrays were photo-patterned in KMPR microwells on fused silica chips using a single-step photo-polymerization process. The new approach of patterning photoresist as the microstructures is more advantageous than developing wells using dry or wet etch on glass materials. A backside exposure step was applied in patterning KMPR 1025, which prominently promoted the adhesion to glass surfaces and provided a promising base with KMPR materials for biological applications. Single cells of interest were selected by a custom-built pico-pump and loaded into 3 × 3 microwells. When the single cells were sealed with the extracellular tri-color sensors in a microchamber by external mechanical force, the performance of the tri-color sensor arrays in metabolic profiling "draw-down" experiments was demonstrated. The demonstration of these improved microfabrication technologies and sensors provides a foundation for

multiparameter analysis of cell respiration and other metabolic parameters at the single-cell, multiple-cell, and tissue level.

In Chapter 3, a microfluidic device was designed, optimized and implemented to measure the oxygen and pH kinetics of live single cells. The configuration is derived from the previously developed "lid-on-top" structures, micro channels were introduced to manipulate rapid cell trapping for 10 × 10 matrix or larger throughput. When single cells in bulk solution flowed through the micro channels, a 95 cells were immobilized by the Pachinko-shaped traps in a very short time (30 – 60 seconds) compared to the pico-pump. As a result, the design can be expanded to high-throughput screening for single-cell analysis. In addition, the micro channels allowed mineral oil to be utilized as a sealing material when the single cells and optical sensors were assembled in the microfluidic device. According to the demonstrated properties compared among different fluids (such as interfacial tension and spreading coefficient), mineral oil successfully sealed the microchambers. Without depending on large external forces to seal the micro structures, sealing based on mineral oil avoided unexpected cracks by inappropriate force. Similarly, the concentration change of oxygen and pH in local micro-environment of the single cells were reflected by alterations in fluorescence intensities from the optical sensors. The tri-color sensor presented sensitive responses to the varied concentration of the oxygen and pH inside the microchamber. By embedding other types of optical sensors (such as glucose, ATP, K^+), more metabolic parameters can be measured and used to monitor cell status, which benefit to understand cellular heterogeneity. The response of single cells to the drug (CCCP) was also studied on the same cells. The structure mechanism provided different cell culture medium exchange through a 1 micron gap, which allowed drug molecules enter

the microchambers without opening the lid (potentially causing migration of the cells). The platform enabled monitoring the response of individual cells to the drug, which can be useful for drug screening purposes.

In Chapter 4, a thermoplastic replication involved in the single-cell metabolic profiling was demonstrated. The main advantage of applying plastic material is low cost, in terms of the process cost and cost of materials. Compared to the conventional glass fabrication, plastic replication required much less process time and metal mold could be reused for mass production. Therefore, the technique allows to produce single-use chips in large numbers. The cell loading device and draw-down device were almost the same as demonstrated in Chapter 3. The metabolic measurements showed cell-to-cell metabolic alterations in the 10 × 10 cell array on the plastic surface. This approach successfully combined low-cost plastics fabrication with single-cell metabolic analysis.

Contributions of this PhD research:

1. Further developed and optimized an advanced microfluidic device to measure multiple metabolic parameters at the single cell level.
2. Optimized the use of mineral oil as a sealing material integrated into microfluidic devices.
3. Achieved a rapid way to load large numbers of live single cells.
4. Fabricated patterned chips using thermoplastic polymers with low processing time and cost.

5. Applied plastic materials in the single cell metabolic analysis.

6. Monitored live single cells' reactions to drug molecules on the device.

5.2 Future Work

Firstly, multi-parameter analysis at the single-cell level enables an understanding of individual cellular heterogeneity. Although OCR and ECAR reveal very important metabolic parameters in cellular phenotypes, other physiological factors need to be obtained as well, such as glucose consumption, which may be achieved by synthesizing more sensors in one solution or developing deposition procedures to pattern multiple sensors in a particular array. Secondly, currently single cells can be successfully trapped in a 10 × 10 matrix and the mechanism of the configuration can allow the device to be scaled up for high-throughput designs. For example, the device can be further developed to load 1,000 or even 10,000 cells in a very short time. Automation in the draw-down device can be introduced to implement a faster, more reliable assembly. In addition, the current device depends on screws to press the two micro-patterned chips together, while unbalanced forces applied across the surface may cause failed sealing by the mineral oil. The top PMMA lid can be mounted to a computer-controlled XYZ stage for alignment. When a drug is introduced into microfluidic channels, the stage can be slightly lifted up to allow the drug molecules to enter the microchamber. Therefore, with this automated design, a 1 micron gap between the two chips is not necessary in the application.

5.3 Acknowledgment

This work was supported by the NIH National Human Genome Research Institute, Centers of Excellence in Genomic Science (CEGS), Microscale Life Sciences Center, (D. R. Meldrum, PI) and NIH Common Fund projectU01CA164250, Live-Cell Microarray for High-Throughput Observation of Metabolic Signatures, U01CA164250 (D. R. Meldrum, PI). I would like to thank the staff from Center for Solid State Electronic Research, Arizona State University for their technical support on the fabrication processes.

.

REFERENCES

Alderman, J., J. Hynes, S. M. Floyd, J. Krüger, R. O'Connor and D. B. Papkovsky (2004). "A low-volume platform for cell-respirometric screening based on quenched-luminescence oxygen sensing." Biosensors and Bioelectronics **19**(11): 1529-1535.

Anis, Y., J. Houkal, M. Holl, R. Johnson and D. Meldrum (2011). "Diaphragm pico-liter pump for single-cell manipulation." Biomedical Microdevices **13**(4): 651-659.

Beckman, R. A., G. S. Schemmann and C.-H. Yeang (2012). "Impact of genetic dynamics and single-cell heterogeneity on development of nonstandard personalized medicine strategies for cancer." Proceedings of the National Academy of Sciences **109**(36): 14586-14591.

Blanco Carballo, V., J. Melai, C. Salm and J. Schmitz (2008). "Moisture resistance of SU-8 and KMPR as structural material for integrated gaseous detectors."

Cairns, R. A., I. S. Harris and T. W. Mak (2011). "Regulation of cancer cell metabolism." Nature Reviews Cancer **11**(2): 85-95.

Cornelison, D. and B. J. Wold (1997). "Single-cell analysis of regulatory gene expression in quiescent and activated mouse skeletal muscle satellite cells." Developmental biology **191**(2): 270-283.

Diepart, C., J. Verrax, P. B. Calderon, O. Feron, B. F. Jordan and B. Gallez (2010). "Comparison of methods for measuring oxygen consumption in tumor cells in vitro." Analytical biochemistry **396**(2): 250-256.

Dragavon, J., T. Molter, C. Young, T. Strovas, S. McQuaide, M. Holl, M. Zhang, B. Cookson, A. Jen and M. Lidstrom (2008). "A cellular isolation system for real-time single-cell oxygen consumption monitoring." Journal of The Royal Society Interface **5**(Suppl 2): S151-S159.

Dumont, E. and H. Delmas (2003). "Mass transfer enhancement of gas absorption in oil-in-water systems: a review." Chemical Engineering and Processing: Process Intensification **42**(6): 419-438.

Enriquez-Navas, P. M., J. W. Wojtkowiak and R. A. Gatenby (2015). "Application of evolutionary principles to cancer therapy." Cancer research **75**(22): 4675-4680.

Etzkorn, J. R., W.-C. Wu, Z. Tian, P. Kim, S.-H. Jang, D. R. Meldrum, A. K. Jen and B. A. Parviz (2010). "Using micro-patterned sensors and cell self-assembly for measuring the oxygen consumption rate of single cells." Journal of Micromechanics and Microengineering **20**(9): 095017.

Fay, J. A. (1971). Physical processes in the spread of oil on a water surface. International Oil Spill Conference, American Petroleum Institute.

Hameeteman, W., G. Tytgat, H. Houthoff and J. Van Den Tweel (1989). "Barrett's esophagus; development of dysplasia and adenocarcinoma." Gastroenterology **96**(5): 1249-1256.

Howland, R. B. and A. Bernstein (1931). "A method for determining the oxygen consumption of a single cell." The Journal of general physiology **14**(3): 339-348.

Hsu, P. P. and D. M. Sabatini (2008). "Cancer cell metabolism: Warburg and beyond." Cell **134**(5): 703-707.

Irish, J. M., N. Kotecha and G. P. Nolan (2006). "Mapping normal and cancer cell signalling networks: towards single-cell proteomics." Nature Reviews Cancer **6**(2): 146-155.

Kelbauskas, L., S. Ashili, J. Zeng, A. Rezaie, K. Lee, D. Derkach, B. Ueberroth, W. Gao, T. Paulson, H. Wang, Y. Tian, D. Smith, B. Reid and D. R. Meldrum (2017). "Platform for combined analysis of functional and biomolecular phenotypes of the same cell." Scientific Reports **7**: 44636.

Kelbauskas, L., S. P. Ashili, J. Houkal, D. Smith, A. Mohammadreza, K. B. Lee, J. Forrester, A. Kumar, Y. H. Anis and T. G. Paulson (2012). "Method for physiologic phenotype characterization at the single-cell level in non-interacting and interacting cells." Journal of biomedical optics **17**(3): 0370081-03700812.

Kelbauskas, L., H. Glenn, C. Anderson, J. Messner, K. B. Lee, G. Song, J. Houkal, F. Su, L. Zhang and Y. Tian (2017). "A platform for high-throughput bioenergy production phenotype characterization in single cells." Scientific Reports **7**.

Kim, K., D. S. Park, H. M. Lu, W. Che, K. Kim, J.-B. Lee and C. H. Ahn (2004). "A tapered hollow metallic microneedle array using backside exposure of SU-8." Journal of Micromechanics and Microengineering **14**(4): 597.

Koivula, H. M., L. Jalkanen, E. Saukkonen, S.-S. Ovaska, J. Lahti, H. Christophliemk and K. S. Mikkonen (2016). "Machine-coated starch-based dispersion coatings prevent mineral oil migration from paperboard." Progress in Organic Coatings **99**: 173-181.

Lee, C. and K. Jiang (2008). "Fabrication of thick electroforming micro mould using a KMPR negative tone photoresist." Journal of Micromechanics and Microengineering **18**(5): 055032.

Lidstrom, M. E. and M. C. Konopka (2010). "The role of physiological heterogeneity in microbial population behavior." Nature chemical biology **6**(10): 705-712.

Lidstrom, M. E. and D. R. Meldrum (2003). "Life-on-a-chip." Nature Reviews Microbiology **1**(2): 158-164.

Manz, A., D. J. Harrison, E. M. Verpoorte, J. C. Fettinger, A. Paulus, H. Lüdi and H. M. Widmer (1992). "Planar chips technology for miniaturization and integration of separation techniques into monitoring systems: capillary electrophoresis on a chip." Journal of Chromatography A **593**(1-2): 253-258.

Meldrum, D. R. and M. R. Holl (2002). "Microscale bioanalytical systems." Science **297**(5584): 1197-1198.

Molter, T. W., M. R. Holl, J. M. Dragavon, S. C. McQuaide, J. B. Anderson, A. C. Young, L. W. Burgess, M. E. Lidstrom and D. R. Meldrum (2008). "A new approach for measuring single-cell oxygen consumption rates." IEEE Transactions on Automation Science and Engineering **5**(1): 32-42.

Ou, K. S., H. Y. Yan and K. S. Chen (2008). "Mechanical Characterization of KMPR by Nano-Indentation for MEMS Applications." Strain **44**(3): 267-271.

Park, E. J., K. R. Reid, W. Tang, R. T. Kennedy and R. Kopelman (2005). "Ratiometric fiber optic sensors for the detection of inter-and intra-cellular dissolved oxygen." Journal of Materials Chemistry **15**(27-28): 2913-2919.

Peng, Z.-c., Z.-g. Ling, M. Tondra, C.-g. Liu, M. Zhang, K. Lian, J. Goettert and J. Hormes (2006). "CMOS compatible integration of three-dimensional microfluidic systems based on low-temperature transfer of SU-8 films." Journal of Microelectromechanical systems **15**(3): 708-716.

Peterman, M. C., P. Huie, D. Bloom and H. A. Fishman (2003). "Building thick photoresist structures from the bottom up." Journal of Micromechanics and Microengineering **13**(3): 380.

Ray, T., H. Zhu and D. R. Meldrum (2010). "Deep reactive ion etching of fused silica using a single-coated soft mask layer for bio-analytical applications." Journal of Micromechanics and Microengineering **20**(9): 097002.

Rodrigo, P. J., V. R. Daria and J. Glückstad (2004). "Real-time three-dimensional optical micromanipulation of multiple particles and living cells." Optics letters **29**(19): 2270-2272.

Rodrigues, M., D. Meldrum, L. Kelbauskas and J. LaBelle Microfluidic Platform for Multi-parameter Analysis of Live Single Cells. Microfluidic Platform for Multi-parameter Analysis of Live Single Cells, Arizona State University.

Rossier, J., A. Schwarz, F. Bianchi, F. Reymond, R. Ferrigno and H. H. Girault (2000). Polymer micro-structures: prototyping, low-cost mass fabrication and analytical applications. Micro Total Analysis Systems 2000, Springer.

Shaw, M., D. Nawrocki, R. Hurditch and D. Johnson (2003). "Improving the process capability of SU-8." Microsystem Technologies **10**(1): 1-6.

Smallwood, S. A., H. J. Lee, C. Angermueller, F. Krueger, H. Saadeh, J. Peat, S. R. Andrews, O. Stegle, W. Reik and G. Kelsey (2014). "Single-cell genome-wide bisulfite sequencing for assessing epigenetic heterogeneity." Nature methods **11**(8): 817-820.

Snijder, B., R. Sacher, P. Rämö, E.-M. Damm, P. Liberali and L. Pelkmans (2009). "Population context determines cell-to-cell variability in endocytosis and virus infection." Nature **461**(7263): 520-523.

Tian, Y., H. Wang, G. Song, F. Su, L. Zhang, D. Meldrum, L. Kelbauskas and B. Ueberroth (2016). Photo-patternable optical luminescence dual sensors and methods of preparing and using them, Google Patents.

Torres-García, W., S. Ashili, L. Kelbauskas, R. H. Johnson, W. Zhang, G. C. Runger and D. R. Meldrum (2012). "A statistical framework for multiparameter analysis at the single-cell level." Molecular BioSystems **8**(3): 804-817.

Wheeler, A. R., W. R. Throndset, R. J. Whelan, A. M. Leach, R. N. Zare, Y. H. Liao, K. Farrell, I. D. Manger and A. Daridon (2003). "Microfluidic device for single-cell analysis." Analytical chemistry **75**(14): 3581-3586.

Wu, M., A. Neilson, A. L. Swift, R. Moran, J. Tamagnine, D. Parslow, S. Armistead, K. Lemire, J. Orrell and J. Teich (2007). "Multiparameter metabolic analysis reveals a close link between attenuated mitochondrial bioenergetic function and enhanced glycolysis dependency in human tumor cells." American Journal of Physiology-Cell Physiology **292**(1): C125-C136.

Zettlemoyer, A., M. Aronson and J. Lavelle (1970). "Spreading at the teflon/oil/water/air interfaces." Journal of Colloid and Interface Science **34**(4): 545-548.

Zhang, L., F. Su, X. Kong, F. Lee, S. Sher, K. Day, Y. Tian and D. R. Meldrum (2016). "1, 8-Naphthalimide Derivative Dyes with Large Stokes Shifts for Targeting Live-Cell Mitochondria." ChemBioChem **17**(18): 1719-1724.

Zhu, H., M. Holl, T. Ray, S. Bhushan and D. R. Meldrum (2009). "Characterization of deep wet etching of fused silica glass for single cell and optical sensor deposition." Journal of Micromechanics and Microengineering **19**(6): 065013.

Zhu, H., Y. Tian, S. Bhushan, F. Su and D. R. Meldrum (2012). "High throughput micropatterning of optical oxygen sensor for single cell analysis." Sensors Journal, IEEE **12**(6): 1668-1672.

Zhu, H., X. Zhou, F. Su, Y. Tian, S. Ashili, M. R. Holl and D. R. Meldrum (2012). "Micro-patterning and characterization of PHEMA-co-PAM-based optical chemical sensors for lab-on-a-chip applications." Sensors and Actuators B: Chemical **173**: 817-823.